

Comparisons
between g-b FTIR and
MIPAS N₂O and HNO₃

C. Vigouroux et al.

Comparisons between ground-based FTIR and MIPAS N₂O and HNO₃ profiles before and after assimilation in BASCOE

C. Vigouroux¹, M. De Mazière¹, Q. Errera¹, E. Mahieu², P. Duchatelet², S. Wood³, D. Smale³, S. Mikuteit⁴, T. Blumenstock⁴, F. Hase⁴, and N. Jones⁵

¹Belgian Institute for Space Aeronomy (BIRA-IASB), Brussels, Belgium

²Institut d'Astrophysique et de Géophysique, University of Liège (ULg), Liège, Belgium

³National Institute for Water and Atmospheric Research (NIWA), Lauder, Otago, New-Zealand

⁴Institute of Meteorology and Climate Research (IMK), Forschungszentrum Karlsruhe and University of Karlsruhe, Karlsruhe, Germany

⁵University of Wollongong, Wollongong, Australia

Received: 29 May 2006 – Accepted: 10 August 2006 – Published: 1 September 2006

Correspondence to: C. Vigouroux (Corinne.Vigouroux@bira-iasb.oma.be)

Title Page

Abstract

Introduction

Conclusions

References

Tables

Figures

◀

▶

◀

▶

Back

Close

Full Screen / Esc

Printer-friendly Version

Interactive Discussion

Abstract

Within the framework of the Network for Detection of Atmospheric Composition Change (NDACC), regular ground-based Fourier transform infrared (FTIR) measurements of many species are performed at several locations. Inversion schemes provide vertical profile information and characterization of the retrieved products which are therefore relevant for contributing to the validation of MIPAS profiles in the stratosphere and upper troposphere. We have focused on the species HNO_3 and N_2O at 5 NDACC-sites distributed in both hemispheres, i.e., Jungfraujoch (46.5°N) and Kiruna (68°N) for the northern hemisphere, and Wollongong (34°S), Lauder (45°S) and Arrival Heights (78°S) for the southern hemisphere. These ground-based data have been compared with MIPAS offline profiles (v4.61) for the year 2003, collocated within 1000 km around the stations, in the lower to middle stratosphere. To get around the spatial collocation problem, comparisons have also been made between the same ground-based FTIR data and the corresponding profiles resulting from the stratospheric 4D-VAR data assimilation system BASCOE. This paper discusses the results of the comparisons and the usefulness of using BASCOE profiles as proxies for MIPAS data. It shows good agreement between MIPAS and FTIR N_2O partial columns: the biases are below 5% for all the stations and the standard deviations are below 7% for the three mid-latitude stations, and below 10% for the high latitude ones. The comparisons with BASCOE partial columns give standard deviations below 4% for the mid-latitude stations to less than 8% for the high-latitude ones. After making some corrections to take into account the known bias due to the use of different spectroscopic parameters, the comparisons of HNO_3 partial columns show biases below 3% and standard deviations below 15% for all the stations except Arrival Heights (bias of 6%, standard deviation of 21%). The results for this species, which has a larger spatial variability, highlight the necessity of defining appropriate collocation criteria and of accounting for the spread of the observed airmasses. BASCOE appears to have more deficiencies in producing proxies of MIPAS HNO_3 profiles compared to N_2O , but the obtained standard deviation of less

ACPD

6, 8335–8382, 2006

Comparisons between g-b FTIR and MIPAS N_2O and HNO_3

C. Vigouroux et al.

Title Page

Abstract

Introduction

Conclusions

References

Tables

Figures

◀

▶

◀

▶

Back

Close

Full Screen / Esc

Printer-friendly Version

Interactive Discussion

EGU

than 10% between BASCOE and FTIR is reasonable. Similar results on profiles comparisons are also shown in the paper, in addition to partial column ones.

1 Introduction

MIPAS, Michelson Interferometer for Passive Atmospheric Sounding¹ (Fischer and Oelhaf, 1996; ESA, 2000), is one of the 10 instruments on board the European satellite ENVISAT which was launched into a sun-synchronous polar orbit at 800 km altitude, on 1 March 2002. This Fourier transform spectrometer operates in the mid infrared (4.15–14.6 μm or 685–2410 cm^{-1}) and measures high-resolution (better than 0.035 cm^{-1}) radiance spectra at the Earth's limb. It provides day and night vertical profiles of a large number of atmospheric species with a complete global coverage of the Earth obtained in 3 days.

Part of the validation of the MIPAS Level 2 products is performed within the ENVISAT Stratospheric Aircraft and Balloon Campaigns (ESABC) or by comparisons with data from other limb sounding instruments such as HALOE (the HALogen Occultation Experiment on UARS, the Upper Atmosphere Research Satellite²). Additional independent measurements for the validation of MIPAS are performed by the ground-based Fourier transform infrared (FTIR) solar absorption spectrometers, like those operated in the framework of the Network for the Detection of Atmospheric Composition Change (NDACC³, formerly called NDSC, Network for the Detection of Stratospheric Change). The implementation of the Optimal Estimation Method, described in Rodgers (2000), in the inversion schemes of the ground-based FTIR spectra allows the retrieval of low resolution vertical profile information (in addition to the standard total column amounts), and the characterization of the retrieved products. When it comes to verifying the MI-

¹<http://envisat.esa.int/instruments/mipas/>

²<http://haloedata.larc.nasa.gov/home/>

³<http://www.ndacc.org/>

Comparisons between g-b FTIR and MIPAS N₂O and HNO₃

C. Vigouroux et al.

Title Page

Abstract

Introduction

Conclusions

References

Tables

Figures

◀

▶

◀

▶

Back

Close

Full Screen / Esc

Printer-friendly Version

Interactive Discussion

PAS profiles at their full vertical resolution, the FTIR data cannot compete with the high vertical resolution measurements coming from balloon, aircraft or limb sounding satellite experiments. The particular benefit of using ground-based FTIR data lies in the fact that these measurements are performed regularly under clear-sky conditions, at many stations distributed over the globe, and thus represent a very interesting complementary dataset for performing a statistically sound validation, and for monitoring the quality of the MIPAS products on the longer term. These ground-based FTIR data are therefore useful for contributing to the validation of MIPAS profiles in the stratosphere and upper troposphere.

Some preliminary results of MIPAS validation by balloon, aircraft, satellite and ground-based measurements have been presented in the second workshop on Atmospheric Chemistry Validation of Envisat (ACVE-2) in May 2004 for all the MIPAS ESA Level 2 products, that are the vertical profiles of: temperature (Blom et al., 2004; Fricke et al., 2004; Dethof et al., 2004), H₂O (Oelhaf et al., 2004a; Pappalardo et al., 2004; Weber et al., 2004), NO₂ (Wetzel et al., 2004), O₃ (Cortesi et al., 2004; Blumenstock et al., 2004a; Kerridge et al., 2004), CH₄ (Camy-Peyret et al., 2004a), N₂O (Camy-Peyret et al., 2004b), and HNO₃ (Oelhaf et al., 2004b). Some results on MIPAS data assimilation was also shown for H₂O (Lahoz et al., 2004) and O₃ (Fonteyn et al., 2004). In the present study, we focus on a more advanced validation of the MIPAS ESA products for the year 2003, for N₂O and HNO₃, a tropospheric species and a stratospheric species respectively, for which the FTIR technique is the only available ground-based source of data. Five NDACC stations are involved in this work: Kiruna (67.8° N, 20.4° E, altitude 420 m a.s.l.) and Jungfraujoch (46.5° N, 8.0° E, 3580 m a.s.l.) in the northern hemisphere, and Wollongong (34.4° S, 150.9° E, 30 m a.s.l.), Lauder (45.0° S, 169.7° E, 370 m a.s.l.), and Arrival Heights (77.8° S, 166.7° E, 200 m a.s.l.) in the southern hemisphere.

This paper describes in Sect. 2 the MIPAS ESA Level 2 products and, in Sect. 3, the ground-based FTIR vertical profile data, including the retrieval strategies used at each station and the characterization of the data products. BASCOE, a 4D-VAR chem-

**Comparisons
between g-b FTIR and
MIPAS N₂O and HNO₃**C. Vigouroux et al.

Title Page

Abstract

Introduction

Conclusions

References

Tables

Figures

◀

▶

◀

▶

Back

Close

Full Screen / Esc

Printer-friendly Version

Interactive Discussion

ical data assimilation system, is briefly described in Sect. 4. In subsequent section, we explain the adopted methodology for the comparisons for which two approaches have been used. First, we have made the comparisons with the MIPAS offline profiles (v4.61) provided by ESA, taking care to define reasonable collocation criteria that give enough coincidences to obtain relevant statistics. Then, to improve the collocations without decreasing the number of coincidences, we have compared the ground-based FTIR profiles with the products of BASCOE. In the current configuration, BASCOE is constrained with MIPAS data and thus delivers atmospheric profiles that can be considered to be proxies of the MIPAS profiles, at any location and any time. In the last part (Sect. 6), we show the results obtained from the comparisons for both molecules, N₂O and HNO₃, at the different stations, and try to answer the following two questions: (1) can we quantify the agreement between the MIPAS and the ground-based FTIR data, and (2), what are the benefits of using the results of a data assimilation system as proxies of MIPAS profiles instead of the MIPAS profiles themselves?

2 MIPAS data

The MIPAS Level 2 products are described in the MIPAS Product Handbook⁴. The MIPAS offline data used here were provided by the ESA v4.61 data processor (ESA, 2004). They include the N₂O and HNO₃ volume mixing ratio (vmr) profiles as well as the atmospheric pressure and temperature vertical distributions. The vertical resolution of the delivered profiles is between 3 and 4 km and their horizontal resolution is between 300 and 500 km along track.

MIPAS data are valid over variable altitude ranges. We observed that, for the scans used in the present study, the upper limits are quite constant for all profiles and are around 61 km for N₂O and 43 km for HNO₃. The lower limits vary a lot between a minimum of 6 km for N₂O and 8 km for HNO₃ to greater than 20 km for worst cases.

⁴<http://envisat.esa.int/dataproducts/mipas>

Comparisons between g-b FTIR and MIPAS N₂O and HNO₃

C. Vigouroux et al.

Title Page

Abstract

Introduction

Conclusions

References

Tables

Figures

◀

▶

◀

▶

Back

Close

Full Screen / Esc

Printer-friendly Version

Interactive Discussion

For the comparisons between ground-based FTIR and MIPAS measurements, we have rejected MIPAS scans that have a lower limit greater than 12 km for N₂O and 14 km for HNO₃. Because of possible uncertainties in the referencing of the MIPAS profiles versus altitude (Fricke et al., 2004), we have adopted a vertical pressure grid for making the comparisons. The FTIR data are reported on an altitude grid, specific of the station. Daily pressure data from each station have been used to convert the altitude grid to a unique pressure grid. The MIPAS retrieved profiles were interpolated onto the same pressure grid. Beyond the limits of MIPAS measurements, the MIPAS profiles are extrapolated using the MIPAS initial guess profiles.

3 Ground-based FTIR data

3.1 Retrieval algorithms

Vertical profile informations can be obtained from high-resolution FTIR solar occultation spectra thanks to the pressure broadening of the absorption lines which leads to an altitude dependence of the lineshapes. Two different algorithms have been used in the present work, SFIT2 and PROFFIT9. Both codes are based on a semi-empirical implementation of the Optimal Estimation Method developed by Rodgers (2000) and provide the retrieval of molecular vertical profiles by fitting one or more narrow spectral intervals (microwindows). The SFIT2 algorithm has been described in previous works (Pougatchev et al., 1995a,b; Rinsland et al., 1998). It was used for the spectral inversion of the FTIR data at all stations except Kiruna. The profiles of this latter station have been retrieved using the PROFFIT9 algorithm (Hase, 2000). It has been shown recently (Hase et al., 2004) that the retrieved profiles and total column amounts obtained by these two different algorithms under identical conditions are in excellent agreement (within 1% for total column amounts of N₂O and HNO₃).

In both codes SFIT2 and PROFFIT9, the retrieved state vector contains the retrieved volume mixing ratios of the target gas defined in discrete layers in the atmosphere, as

Title Page

Abstract

Introduction

Conclusions

References

Tables

Figures

◀

▶

◀

▶

Back

Close

Full Screen / Esc

Printer-friendly Version

Interactive Discussion

well as the retrieved scaling factors for the interfering species column amounts, and fitted values for some model parameters. These can include the baseline slope and instrumental lineshape parameters such as an effective apodization. For the stations Jungfraujoch, Wollongong, Lauder and Arrival Heights, the atmosphere is divided in 29 layers, whereas for Kiruna it is divided in 44 layers. The 29 layers have a width of 2 km below 50 km, becoming progressively larger towards the top of the atmosphere, defined here as 100 km. The widths of the 44 layers of Kiruna progressively grow from 0.4 km at the ground to 2.3 km around 50 km altitude.

3.2 Retrieval parameters

3.2.1 Spectroscopic data and spectral windows

All stations are using the spectroscopic line parameters from the HITRAN 2000 database including official updates through 2001 (Rothman, 2003). Wollongong added official updates up to August 2002 and additional lines from the Spectroscopic Atlas of Atmospheric Microwindows in the Middle Infra-Red (2nd edition) (Meier et al., 2004) but these do not include changes in the parameters for N₂O or HNO₃, or for the six interfering species, given in Table 1, that are fitted in Wollongong retrievals.

At all stations daily temperature and pressure profiles have been taken from the National Centers for Environmental Prediction (NCEP).

The retrieval microwindows used at the various stations are listed in Table 1, together with the corresponding interfering species. The a priori profiles of these interfering species are scaled simultaneously with the profile inversion of the target gases in the spectral fit procedure.

3.2.2 A priori information

Because the inversion problem is ill-posed, the Optimal Estimation Method needs some a priori information about the retrieval state vector parameters, including the a priori

Comparisons between g-b FTIR and MIPAS N₂O and HNO₃

C. Vigouroux et al.

Title Page

Abstract

Introduction

Conclusions

References

Tables

Figures

◀

▶

◀

▶

Back

Close

Full Screen / Esc

Printer-friendly Version

Interactive Discussion

vertical vmr profile x_a , and the associated a priori covariance matrix \mathbf{S}_a (Rodgers, 2000).

In Fig. 1, we show the a priori N_2O and HNO_3 vertical profiles used at each station. For the stations Jungfraujoch, Lauder, Arrival Heights and Wollongong, the a priori profiles have been taken identical to the climatological initial guess profiles from MIPAS for the corresponding seasons and latitude bands (so-called IG2 profiles in the MIPAS Product Handbook). Three different seasonal profiles are used, representative of the periods January to March, April to September and October to December. For the Kiruna station, only one a priori profile is used for each species, namely the MIPAS IG2 profile for the April to September season corresponding to the latitude of Kiruna. For HNO_3 at Kiruna, the MIPAS IG2 profile has been modified below 30 km because it was found more realistic to enhance the a priori amount of HNO_3 near the tropopause.

3.3 Characterization of the retrievals

As discussed in Rodgers (2000), the Optimal Estimation Method allows the characterization of the retrievals, i.e., the vertical resolution of the retrieval, its sensitivity to the a priori information and the degrees of freedom for signal (DOFS). This is obtained by considering that the retrieved state vector x_r is related to the true state vector x by:

$$x_r = x_a + \mathbf{A}(x - x_a) + \text{error terms},$$

with x_a the a priori state vector and \mathbf{A} the matrix whose rows are called the averaging kernels. The retrieved parameters are weighted means of the true and a priori state vector parameters. The weight associated with the true state vector parameters is given by the averaging kernels matrix \mathbf{A} which would be the identity matrix in an ideal case where the retrieval would reproduce the truth. The actual averaging kernels matrix depends on several parameters including the solar zenith angle, the spectral resolution and signal to noise ratio, the choice of retrieval spectral microwindows, and the a priori covariance matrix \mathbf{S}_a . The elements of the averaging kernel for a given altitude give the sensitivity of the retrieved profile at that altitude to the real profile at each altitude,

Comparisons between g-b FTIR and MIPAS N_2O and HNO_3

C. Vigouroux et al.

Title Page

Abstract

Introduction

Conclusions

References

Tables

Figures

◀

▶

◀

▶

Back

Close

Full Screen / Esc

Printer-friendly Version

Interactive Discussion

and its full width at half maximum is a measure of the vertical resolution of the retrieval at that altitude. Figures 2 and 3 show the mean averaging kernels for N₂O at Arrival Heights and for HNO₃ at Lauder, respectively. We see that the best vertical resolution is approximately 8 km for N₂O and 10 km for HNO₃.

5 The DOFS of the ground-based retrievals are given by the trace of the averaging kernel matrix **A**. Thus, they depend on the parameters given previously, which can be different for each station and each spectrum. We have calculated, for each station, their mean value for the data used in this study. We list them for both molecules in Table 2: for HNO₃ they vary from 1.9 at the Jungfraujoch station to 2.8 at Lauder, whereas for
10 N₂O they vary from 4.3 at the Jungfraujoch, thanks to the highest altitude of this station, to 3.5 at Wollongong.

On top of the kernels plotted in Figs. 2 and 3, we have added the so-called “sensitivity” of the retrievals at each altitude to the measurements. This sensitivity at altitude *k* is calculated as the sum of the elements of the corresponding averaging kernel, $\sum_i A_{ki}$.
15 It indicates, at each altitude, the fraction of the retrieval that comes from the measurement rather than from the a priori information. A value larger than one means that the retrieved profile at that altitude is over-sensitive to changes in the real profile. It may be compensating for poor sensitivity to the true profile at other altitudes when the averaging kernels do not allow the separation of the altitude ranges correctly. A value close
20 to zero at a certain altitude indicates that the retrieved profile at that altitude is nearly independent of the real profile and is therefore approaching the a priori profile. In other words, the measurements have not significantly contributed to the retrieved profile at that altitude.

25 Figure 2 shows that the ground-based FTIR measurements of N₂O at Arrival Heights have a sensitivity larger than 0.5 from the ground to about 30 km altitude. For the HNO₃ retrievals at Lauder, the measurements have the largest sensitivity between 10 and 35 km, as shown in Fig. 3. The altitude range with better sensitivity does not only depend on the species considered, but it is also different at the various stations in agreement with the different degrees of freedom given in Table 2.

**Comparisons
between g-b FTIR and
MIPAS N₂O and HNO₃**C. Vigouroux et al.

Title Page

Abstract

Introduction

Conclusions

References

Tables

Figures

⏪

⏩

◀

▶

Back

Close

Full Screen / Esc

Printer-friendly Version

Interactive Discussion

For making relevant comparisons between the ground-based and satellite data, we focus on the altitude ranges in which the sensitivity of the retrieved profiles to the measurements is sufficiently high. As we intend to compare partial column amounts in addition to the profile comparisons, we have adopted a strict criterion to define the altitude boundaries of these partial columns: the sensitivity, as defined above, must be larger than 0.5, which means that the retrieved profile information comes for more than 50% from the measurement, or, in other words, that the a priori information influences the retrieval for less than 50%. We have added in Table 2 these vertical ranges for each molecule at each station.

4 BASCOE analyses

BASCOE (Belgian Assimilation System of Chemical Observations from ENVISAT⁵) is a 4D-VAR data assimilation system derived from that described in Errera and Fonteyn (2001). This system is based on a 3-D chemical transport model driven by operational ECMWF analysis (Chabrillat et al., 2006⁶ and Daerden et al., 2006⁷). MIPAS v4.61 observations of H₂O, NO₂, O₃, CH₄, N₂O, and HNO₃ have been assimilated for the year 2003. BASCOE ozone analyses have already been validated by Geer et al. (2006) who made intercomparisons of ozone analyses from different assimilation systems, including BASCOE.

The model calculates the evolution of 57 chemical species taking into account the advection, the chemistry and the PSC microphysics. Two configurations of BASCOE are possible (Chabrillat et al., 2006⁶): one with full PSC microphysics and another one

⁵<http://bascoe.oma.be/>

⁶Chabrillat, S. H., Van Roozendaal, M., Daerden, F., et al.: Quantitative assessment of 3-D PSC-chemistry-transport models by simulation of GOME observations during the Antarctic winter of 2002, Atmos. Chem. Phys. Discuss., in preparation, 2006.

⁷Daerden, F., Larsen, N., Bonjean, S., et al.: Synoptic PSCs in recent polar winters: simulations and comparison to observations, Atmos. Chem. Phys. Discuss., submitted, 2006.

Comparisons
between g-b FTIR and
MIPAS N₂O and HNO₃

C. Vigouroux et al.

Title Page

Abstract

Introduction

Conclusions

References

Tables

Figures

◀

▶

◀

▶

Back

Close

Full Screen / Esc

Printer-friendly Version

Interactive Discussion

with PSC parameterization. This study uses BASCOE analyses obtained by the second configuration. The model extends from the surface up to 0.1 hPa using 37 levels with a horizontal resolution of 5° in longitude and 3.75° in latitude. Data assimilation is done using 4D-VAR with an assimilation window of one day. The background error standard deviation is set to 20% of the background field. Correlations are not taken into account and the background covariance matrix is therefore diagonal. Additional to the MIPAS random error, a representation error of 8.5% that takes into account the difference of resolution between BASCOE and MIPAS has been specified for each assimilated observation (Ménard et al., 2000). In order to prevent oscillating data entering into BASCOE, only values in the range [0.2, 200] hPa and [4, 200] hPa are considered for N₂O and HNO₃, respectively (M. Ridolfi, private communication).

In order to evaluate how well BASCOE represents MIPAS, we plot, in Fig. 4, the monthly mean bias ($\langle \text{BASCOE-MIPAS} \rangle / \langle \text{MIPAS} \rangle$) and standard deviation (1σ) between BASCOE and MIPAS profiles of N₂O and HNO₃ in five 10° latitude bands corresponding to each station. Generally, monthly mean N₂O biases are lower than $\pm 5\%$. For some months, higher values are observed in the middle-high stratosphere: above 20 hPa around 75°S, above 5 hPa around 35°S and 65°N and above 3 hPa around 45°S and 45°N. However, these cases occur in pressure ranges outside the limits used to compare FTIR and MIPAS, except for the Jungfraujoch station. For the latter case, one should not take into account profiles comparison with BASCOE for pressures above 3 hPa. The effect on the comparison of partial columns of N₂O above 3 hPa is negligible, since there is almost no N₂O at high altitude (see Fig. 1). Standard deviations of monthly N₂O comparisons are between 10% to 20% within the pressure limits of the comparisons between FTIR and MIPAS, except for Arrival Heights during local winter. We also observe a significant variability from month to month. Nevertheless, this variability is comparable to the estimated assimilation error (random and representativeness errors).

For HNO₃, monthly mean biases are generally negative (BASCOE underestimates MIPAS) and vary with altitude, latitude and month. The bias is minimal, within $\pm 5\%$,

**Comparisons
between g-b FTIR and
MIPAS N₂O and HNO₃**C. Vigouroux et al.

Title Page

Abstract

Introduction

Conclusions

References

Tables

Figures

◀

▶

◀

▶

Back

Close

Full Screen / Esc

Printer-friendly Version

Interactive Discussion

around 80 hPa in the -80 to -70° latitude band, and around 100 hPa in the other latitude bands. The biases are largest at 150 hPa and between 10 and 20 hPa, and vary from month to month between -10% and -30% for the worst case of Arrival Heights during local winter. Regarding the standard deviation, it is minimum around 50 hPa, the altitude at which the HNO_3 mixing ratio reaches its maximum. Within the pressure limits of the comparisons between FTIR and MIPAS, its value lies between 5% and 20% except at the South Pole where it can reach 25% in wintertime. Again, this variability is comparable to the estimated assimilation error.

Having the above statistics in mind, we can evaluate to which extent BASCOE is a proxy of MIPAS. In the case of N_2O , we can say that BASCOE is a good proxy of MIPAS, because the bias between both is negligible. However, it is clear that BASCOE HNO_3 cannot be considered as a good absolute proxy of MIPAS because of the fact that BASCOE underestimates MIPAS HNO_3 . This must be kept in mind when BASCOE will be compared to ground-based FTIR. The origin of this bias has not yet been clearly identified but one possible explanation is the following. In the assimilation system, observations of species will influence initial concentrations of other constituents if they are coupled in the chemical scheme. The fact that HNO_3 observations are assimilated together with other species, in particular O_3 and NO_2 , and the possibility that MIPAS observations of these three species do not agree with the chemical equilibrium conditions in BASCOE, could explain the HNO_3 bias.

5 Comparison methodologies

5.1 Degradation of the MIPAS and BASCOE profiles to the ground-based FTIR resolution

When making intercomparisons of remote sounders having different vertical resolutions, one can use the method given by [Rodgers and Connor \(2003\)](#) to account for that difference. In the present case, the vertical resolution of the MIPAS data is much

Comparisons between g-b FTIR and MIPAS N_2O and HNO_3

C. Vigouroux et al.

Title Page

Abstract

Introduction

Conclusions

References

Tables

Figures

◀

▶

◀

▶

Back

Close

Full Screen / Esc

Printer-friendly Version

Interactive Discussion

higher than that of the ground-based FTIR data. Therefore the MIPAS profiles x_m are considered to be ideal profiles compared to ground-based FTIR ones, and the averaging kernel matrix of MIPAS retrievals is approximated by the identity matrix. Before comparing MIPAS profiles to the ground-based ones, we smoothed them according to the characteristics of the ground-based data, following:

$$x_s = x_a + \mathbf{A}(x_m - x_a), \quad (1)$$

in which x_s are the smoothed MIPAS profiles and x_a and \mathbf{A} are the a priori profile and the averaging kernel matrix of the ground-based FTIR retrievals, respectively.

The same degradation is made for the BASCOE profiles.

Having adopted this approach, the smoothing error must no longer be accounted for in the uncertainties that are to be considered in the comparison results.

From here onwards, we will use the terms MIPAS and BASCOE profiles for the smoothed profiles. The partial columns amounts that are discussed in the paper have been calculated from the smoothed profiles.

5.2 Statistical sets of comparisons

The four statistics defined hereinafter will be described by the mean value of the differences (the “bias”) between MIPAS and FTIR and their standard deviation (1σ) (the “scatter”), in percent. To do so, we divide the mean value and the standard deviation of the absolute differences of partial columns and profiles by the mean of the FTIR partial columns and profiles, respectively. The mean value and standard deviation of our statistics are thus referring to $[\langle \text{MIPAS-FTIR} \rangle \pm 1\sigma] / \langle \text{FTIR} \rangle$ in the tables and figures of Sect. 6. The scatter will be compared to the estimated random error on the differences to discuss the agreement between both instruments. A bias between MIPAS and FTIR will be called “statistically significant” if the mean $\langle \text{MIPAS-FTIR} \rangle$ is larger than the error on that mean, i.e., larger than $3 * \sigma / \sqrt{N}$, with N the number of coincidences.

Comparisons between g-b FTIR and MIPAS N₂O and HNO₃

C. Vigouroux et al.

Title Page

Abstract

Introduction

Conclusions

References

Tables

Figures

◀

▶

◀

▶

Back

Close

Full Screen / Esc

Printer-friendly Version

Interactive Discussion

5.2.1 Comparisons between MIPAS and ground-based profiles for two different collocation criteria

In order to obtain a statistically significant set of comparisons between the MIPAS and ground-based data, we have chosen spatial collocation circles of 1000 km radius around each of the ground-based stations. As the MIPAS tangent point can move by more than 200 km in the horizontal direction during one scan, the criterion is applied such that at least one tangent point of the scan must lie within the collocation circle. The requirement on temporal coincidence is that the recording time difference between the MIPAS and FTIR profile is smaller than 3 h. Each individual MIPAS profile is compared to the mean of the FTIR profiles that are within ± 3 h from the MIPAS measurement time. It is justified to take the mean of the ground-based measurements as the concentrations of N_2O and HNO_3 are not expected to change in such a short lapse of time. Anyway, when the standard deviation of the FTIR data set within these 6 h periods is larger than the estimated random error of the FTIR measurements, we reject that coincidence from our comparison data set. We do not take the mean of the MIPAS scans because their spatial locations and the quality of the profiles can be very different. We have not applied any additional coincidence criterion as to the potential vorticity of the air masses. This leads to larger scatter in the comparisons at the two high latitude stations as will be seen in Sect. 6. This set of comparisons will be called “Statistics 1” in the paper.

To evaluate the impact of the collocation criterion, we will also show the results of comparisons of partial columns for a collocation of 400 km radius, with the additional requirement that all tangent points of the scan must be within the 400 km radius (“Statistics 2”). The same temporal criterion of ± 3 h is used in “Statistics 2”.

The latter collocation choice leads to very poor statistics. To get around the problem of collocation, we have introduced the use of profiles obtained by the 4D-VAR data assimilation system BASCOE which can be seen as proxies of MIPAS profiles, for the

Comparisons between g-b FTIR and MIPAS N_2O and HNO_3

C. Vigouroux et al.

Title Page

Abstract

Introduction

Conclusions

References

Tables

Figures

◀

▶

◀

▶

Back

Close

Full Screen / Esc

Printer-friendly Version

Interactive Discussion

species, altitude ranges and periods discussed in Sect. 4.

5.2.2 Two sets of comparisons using the 4D-VAR data assimilation system BASCOE

For the purpose of this work, BASCOE analyses have delivered vertical profiles of N₂O and HNO₃, at the location of each station, four times a day, namely at 00:00 h, 06:00 h, 12:00 h and 18:00 h UT. The comparisons between the ground-based FTIR and BASCOE data are divided in two sets. “Statistics 3” compares the means of the FTIR data sets involved in “Statistics 1”, not with the collocated MIPAS profiles themselves, but with the BASCOE profiles at the location of the station that are closest in time.

To enlarge the statistics for the comparisons, we also compare the BASCOE profiles with the means of the ground-based FTIR data that are available within the six hours time ranges centered around the times of the BASCOE profiles, even if no correlative MIPAS measurements are available in these periods. This set of comparisons is referred to hereafter as “Statistics 4”.

5.3 Evaluation of data uncertainties

We have evaluated the random error covariance matrix on the difference MIPAS-FTIR using the work of [Rodgers and Connor \(2003\)](#) for the intercomparison of remote sounding instruments, and of [Calisesi et al. \(2005\)](#) for the regridding between the MIPAS and the FTIR data. As seen before, MIPAS profiles have a much higher vertical resolution than ground-based FTIR profiles, so the random error covariance matrix of the comparison MIPAS-FTIR, $\mathbf{S}_{\delta_{12}}$ in Eq. (22) of [Calisesi et al. \(2005\)](#), becomes simply:

$$\mathbf{S}_{\delta_{12}} = \mathbf{S}_{x_1} + \mathbf{A} \mathbf{W}_{12} \mathbf{S}_{x_2} \mathbf{W}_{12}^T \mathbf{A}^T. \quad (2)$$

Herein \mathbf{S}_{x_1} is the random error covariance matrix of the ground-based FTIR retrieved profile x_1 , \mathbf{A} is the FTIR averaging kernel matrix specified on the FTIR retrieval grid, and \mathbf{S}_{x_2} is the random error covariance matrix of the MIPAS profile x_2 specified on the

**Comparisons
between g-b FTIR and
MIPAS N₂O and HNO₃**

C. Vigouroux et al.

Title Page

Abstract

Introduction

Conclusions

References

Tables

Figures

◀

▶

◀

▶

Back

Close

Full Screen / Esc

Printer-friendly Version

Interactive Discussion

MIPAS retrieval grid. \mathbf{W}_{12} is a grid transformation matrix, defined by:

$$\mathbf{W}_{12} = \mathbf{W}_1^* \mathbf{W}_2, \quad (3)$$

with \mathbf{W}_1 and \mathbf{W}_2 the transformation matrices of the FTIR and MIPAS retrieval products x_1 and x_2 to the equivalent retrieval products y_1 and y_2 , respectively, on the same fine grid:

$$y_2 = bfW_2x_2 \quad (4)$$

$$x_1 = \mathbf{W}_1^* y_1. \quad (5)$$

\mathbf{W}_1^* is the generalized pseudo-inverse of \mathbf{W}_1 .

The random error matrix \mathbf{S}_{x_1} for the ground-based FTIR data has been evaluated for a typical measurement at Kiruna with a solar zenith angle of 70° (F. Hase, private communication). For N_2O , the random error matrix is dominated by the contributions from the baseline error, as well as the temperature profile uncertainties. For HNO_3 , the spectral noise is also a dominant error source. Figure 5 shows the square-root of the variances of \mathbf{S}_{x_1} for the FTIR N_2O and HNO_3 retrievals at the Kiruna station.

The ESA MIPAS products include individual error covariance matrices with each profile: they represent the errors due to the noise. As only a typical value is used for the ground-based FTIR uncertainty, we have taken for the MIPAS error covariance matrix due to noise, \mathbf{S}_n , the mean of the matrices corresponding to all the MIPAS scans collocated within 1000 km around the stations.

An analysis of the various other sources of error of the MIPAS retrievals has been made by the Atmospheric, Oceanic and Planetary Physics (AOPP) research team at Oxford University⁸. The systematic errors given by AOPP are typical ones for large latitude bands. These errors are given in percent in an altitude grid, and it is assumed that there are no correlations between errors, i.e., each systematic error covariance matrix is diagonal. The systematic errors are divided into two parts: purely systematic errors and systematic errors with random variability. For the discussion about the

⁸<http://www.atm.ox.ac.uk/group/mipas/err/>

Comparisons
between g-b FTIR and
MIPAS N_2O and HNO_3

C. Vigouroux et al.

Title Page

Abstract

Introduction

Conclusions

References

Tables

Figures

◀

▶

◀

▶

Back

Close

Full Screen / Esc

Printer-friendly Version

Interactive Discussion

Comparisons between g-b FTIR and MIPAS N₂O and HNO₃

C. Vigouroux et al.

Title Page

Abstract

Introduction

Conclusions

References

Tables

Figures

◀

▶

◀

▶

Back

Close

Full Screen / Esc

Printer-friendly Version

Interactive Discussion

scatter of the comparisons, we are interested only in the random error sources (noise and systematic errors with random variability, namely: propagation of temperature random error on the retrievals, horizontal gradient effects, uncertainties on the profiles of interfering species and on the high-altitude column). Hereinafter, we'll designate this random error by the short term “uncertainty”. The total error covariance matrix due to all systematic error sources with random variability, $\mathbf{S}_{\text{sys_rand}}$, has been calculated as the mean of the set of individual matrices in vmr units, obtained from the multiplication of the typical matrix in percentage with the individual MIPAS profile for each coincidence case.

Then the contribution of the MIPAS uncertainties to the combined random error covariance matrix $\mathbf{S}_{\delta_{12}}$ in Eq. (2) is simply: $\mathbf{S}_{x_2} = \mathbf{S}_n + \mathbf{S}_{\text{sys_rand}}$.

Figure 5 shows the square-root of the variances of the smoothed MIPAS profile uncertainty matrix \mathbf{S}_{x_2} for the N₂O and HNO₃ retrievals obtained around the Kiruna station, together with the square-root of the variances of \mathbf{S}_{x_1} and $\mathbf{S}_{\delta_{12}}$ for the FTIR profile and for the absolute difference MIPAS-FTIR, respectively.

In the next section, the random error on the difference between MIPAS and FTIR profiles, i.e., the square-root of the variances of $\mathbf{S}_{\delta_{12}}$, will be represented by the shaded areas around the statistical means of the MIPAS-FTIR difference profiles, in Figs. 8 and 11. As we have decided to show relative differences, the absolute errors have been divided by the mean of the FTIR profiles.

From the error covariance matrix of the difference MIPAS-FTIR, we have calculated the error $\Delta_{\delta_{PC}}$ associated with the difference of partial columns. This calculation is made according to:

$$\Delta_{\delta_{PC}} = \mathbf{g}^T \mathbf{S}_{\delta_{12}} \mathbf{g}, \quad (6)$$

in which \mathbf{g} is the operator that transforms the volume mixing ratio profile in a partial column amount, between the boundaries that have been defined earlier (Sects. 3.3 and 4; see also Tables 3 and 5).

Since we discuss the results of the statistical evaluations in percentage values, in Tables 3 and 5, we calculate the relative error on the partial column differences by

dividing the absolute error (Eq. 6) by the mean of the FTIR partial columns. This relative random error on the difference between MIPAS and FTIR partial columns is given in Tables 3 and 5, and will be compared to the standard deviations of the comparisons statistics to verify whether both instruments are in agreement. This is the subject of the next section.

6 Results of the intercomparisons

6.1 Results for N₂O

6.1.1 Comparisons of the partial columns of N₂O

Table 3 summarizes, for each station, the statistical results of the comparisons of the partial columns of N₂O for the four sets described in Sect. 5.2. As seen in Sect. 2, the vertical coordinate for the comparisons must be pressure rather than altitude. The pressure limits of the partial columns are included in Table 3. The higher pressure limit corresponds to about 12 km (see the discussion on MIPAS observed lower altitudes in Sect. 2) and the lower pressure limit is derived from the FTIR sensitivity (see Table 2).

We have decided to reject the MIPAS scans that do not cover these altitude ranges, the partial columns used in the statistics are therefore not contaminated by some extrapolations with a priori profiles. However, some scans can have one or two missing values that are replaced by interpolated values in the profiles.

Table 3 shows that there is a good agreement between MIPAS and ground-based FTIR partial columns even with the less constrained collocation criteria (“Statistics 1”). For Kiruna, Jungfraujoch and Lauder, there is no statistically significant bias between the two instruments considering the means and their error (about 2%, calculated as explained in Sect. 5) for “Statistics 1”. A small positive bias of $4\pm 2\%$ is obtained at Wollongong, and a negative one of $-5\pm 2\%$ at Arrival Heights. The random errors of the relative differences of partial columns, estimated as seen in Sect. 5.3, are about 6

Comparisons between g-b FTIR and MIPAS N₂O and HNO₃

C. Vigouroux et al.

Title Page

Abstract

Introduction

Conclusions

References

Tables

Figures

◀

▶

◀

▶

Back

Close

Full Screen / Esc

Printer-friendly Version

Interactive Discussion

or 7% as indicated in the table. Agreement between both instruments should give a standard deviation of the statistics similar to the estimated random errors. One expects that the remaining discrepancies of a few percent between the two instruments are due to spatial collocation criteria that are too wide. “Statistics 2”, made with a reduced collocation criterion of 400 km, have indeed lower standard deviations for the three stations where the number of coincidences remains statistically significant (≥ 10).

The reason why the standard deviation of the statistics is not reduced at the Kiruna station by using a stricter collocation criteria can be understood from the timeseries of the partial columns of N_2O in this particular case, as shown in Fig. 6. We see that the variation of the N_2O abundances is much higher during the winter-spring period (January to end of March), probably related to subsidence in polar vortex conditions. Thus, the higher standard deviation of 9% at Kiruna for “Statistics 1” is due to the higher variability of N_2O in time and space, making the collocation criterion less adequate for selecting comparable quantities. The standard deviation remains high (9%) even if the spatial collocation is set to 400 km, probably because in spring even a collocation of 400 km is not sufficient to take into account the N_2O spatial variability during this period. We can however not conclude because of the bad statistical conditions (only six coincidences, two of them occurring in spring).

At the Wollongong station also, “Statistics 2” suffers from a very small number of coincidences, in which essentially one out of the four MIPAS scans in coincidence, in early March, is causing the large value of the standard deviation (10%). Eliminating this point reduces the bias and the standard deviation to $4\pm 3\%$.

A similar problem to Kiruna is encountered at the Arrival Heights station as seen in Fig. 7, with a high variability of N_2O in local spring (September to end of November), thus giving rise to standard deviations of “Statistics 1” and “2” (10% and 9%, respectively) that are high compared to the random error of 6%. To confirm this interpretation, the statistics of the comparisons (relative differences between FTIR and MIPAS partial column values) at Kiruna and Arrival Heights, limited to the local summer-autumn period, are given in Table 4. They show values for the standard deviations that are in

**Comparisons
between g-b FTIR and
MIPAS N_2O and HNO_3** C. Vigouroux et al.

Title Page

Abstract

Introduction

Conclusions

References

Tables

Figures

◀

▶

◀

▶

Back

Close

Full Screen / Esc

Printer-friendly Version

Interactive Discussion

agreement with the expected uncertainty for the relative differences, and that decrease from “Statistics 1” to “Statistics 2”.

As said before, for the purpose of evaluating the impact of the collocation criteria on the comparison results, we have also compared the FTIR data with correlative data from BASCOE analyses, i.e., BASCOE analyses interpolated at the location of the ground stations as proxies for perfectly collocated MIPAS measurements, in “Statistics 3” and “4”. A comparison in Table 3 of the results for “Statistics 1” to those for “Statistics 3”, which include identical sets of FTIR measurements, shows lower standard deviations in the latter case, especially for the three mid-latitudes stations. A similar reduction in the standard deviations is observed in Table 4 for the two high latitude stations, Kiruna and Arrival Heights, when the reduced time period is considered. One also notices very small differences between the results (means and standard deviations) of “Statistics 3” and “Statistics 4” where BASCOE products are used even when there are no MIPAS observations that satisfy the temporal and spatial collocation criteria with the FTIR measurements. These results confirm that BASCOE products can be used reliably as proxies of MIPAS observations at any time within the considered periods.

Still, in the winter-spring periods at high latitudes, where the spatial (and temporal) variability of the N₂O partial column abundances is high, it appears that BASCOE, with its resolution of 5° in longitude and 3.75° in latitude, has more difficulties to correctly capture this variability: the standard deviations of “Statistics 3” or “4” do not go down to the level of the random uncertainty (except “Statistics 3” for Arrival Heights). This is in agreement with Fig. 4 which shows that the standard deviations of the statistics comparing BASCOE and MIPAS are larger for the months January to March at Kiruna, and September to November for Arrival Heights.

One could also notice that the comparisons of BASCOE and FTIR show a significant bias only for Arrival Heights, when the whole period January to December 2003 is considered.

From the best cases (mid-latitude stations) of Table 3 and from Table 4, we see that

**Comparisons
between g-b FTIR and
MIPAS N₂O and HNO₃**

C. Vigouroux et al.

Title Page

Abstract

Introduction

Conclusions

References

Tables

Figures

◀

▶

◀

▶

Back

Close

Full Screen / Esc

Printer-friendly Version

Interactive Discussion

the statistical standard deviations of the observed partial column differences can be slightly smaller than the estimated random uncertainties associated with them. This could lead to the conclusion that the uncertainty estimates for the FTIR profiles are conservative. However, we'll see in the profile comparisons in the next section that the ratio between the statistical standard deviation and the random error varies a lot with altitude (Fig. 8). The overestimation of the random error appears only in the troposphere and lower stratosphere where the amount of N₂O is important.

6.1.2 Comparisons of the vertical profiles of N₂O

Figure 8 shows the statistical means and associated standard deviations of the relative differences between the vertical profiles of N₂O from the ground-based FTIR observations and MIPAS v4.61 ("Statistics 1") and BASCOE products ("Statistics 3"), at the five contributing stations.

The black horizontal bars in Fig. 8 indicate the pressure limits of the partial columns defined in Table 3. As stated before, the MIPAS profiles are extrapolated with the MIPAS initial guess (IG2) values outside the vertical ranges of the measurements. The ground-based FTIR profiles and the smoothed MIPAS profiles tend towards the a priori profiles at altitudes where the sensitivity of the retrievals to the measurements tends to zero. This explains why the relative difference profiles and associated errors all tend to zero at high altitudes.

For Kiruna, we see in Fig. 8 a positive bias (below 3%) between MIPAS and FTIR at low altitudes becoming negative (below 5%) for pressure smaller than 100 hPa. This behaviour is similar for both whole and reduced periods. Considering the error on the mean of the differences (not plotted here, but calculated as discussed in Sect. 5), this bias is statistically significant only for pressure below 80 hPa. The same kind of shape is seen at Lauder, the higher positive bias at low altitude (below 4%) being also statistically significant. At Jungfraujoch, the bias is positive (below 4%) for pressure greater than 40 hPa and become negative above (below 5%, for pressure greater than 20 hPa; below 10% above). At Wollongong, a high positive bias is observed (below 5%

Comparisons between g-b FTIR and MIPAS N₂O and HNO₃

C. Vigouroux et al.

Title Page

Abstract

Introduction

Conclusions

References

Tables

Figures

◀

▶

◀

▶

Back

Close

Full Screen / Esc

Printer-friendly Version

Interactive Discussion

for pressure greater than 55 hPa with a maximum of 21% at 25 hPa). At Arrival Heights a positive significant bias is seen for the whole altitude range, below 8% and 5% for the whole and reduced period, respectively. The shape of the bias look very similar for both compared data sets, MIPAS and BASCOE, confirming what has been seen in Fig. 4, and showing also that they are probably not related to collocation issues, but rather to the shapes of the FTIR retrievals. As the DOFS for the FTIR N₂O retrievals between the considered pressure limits is between 1.3 (Kiruna) and 2.7 (for Jungfraujoch), the detailed shape of the FTIR profiles strongly depends on the retrieval settings.

As seen with the partial columns comparisons in Table 3, the standard deviations of the relative differences are reduced when using collocated BASCOE products instead of the correlative MIPAS data. When comparing the random error and the statistical standard deviations, one should consider that the error calculation has been made using a typical case at Kiruna where the sensitivity is below 0.5 for altitudes greater than 25 km (Table 2). We observe that the statistical standard deviations are lower than the estimated random error for pressures greater than 100 hPa (around 15.5 km), in the troposphere and low stratosphere, where the N₂O amount is important.

6.2 Results for HNO₃

6.2.1 Comparisons of the partial columns of HNO₃

Analogous to the presentation for N₂O in Table 3, Table 5 gives the statistical results, at each station, for the comparisons between FTIR and MIPAS or BASCOE HNO₃ partial column values, according to the four statistical approaches described in Sect. 5.2. The partial column limits (in pressure units) are also included in the second column of Table 5.

The first striking observation is that there exists a negative bias between the FTIR and MIPAS data, of order 11 to 19%. It has already been observed in previous work (Oelhaf et al., 2004b; Blumenstock et al., 2004b) and explained by a scaling factor of 13% that was applied to the HNO₃ line intensities in the spectroscopic data base used

Comparisons between g-b FTIR and MIPAS N₂O and HNO₃

C. Vigouroux et al.

Title Page

Abstract

Introduction

Conclusions

References

Tables

Figures

◀

▶

◀

▶

Back

Close

Full Screen / Esc

Printer-friendly Version

Interactive Discussion

for the MIPAS v4.61 retrievals as compared to the databases used for the ground-based FTIR retrievals (see Sect. 3.2.1). If the same spectroscopy would have been adopted for the MIPAS and FTIR retrievals, the remaining biases, after a correction of 13%, would not have been statistically significant except for Arrival Heights. At the latter station, a positive bias of 6% would still be significant compared to the error on the mean of 4%.

In the case of HNO_3 , the use of BASCOE analyses as proxies for the MIPAS data appears to be more problematic when one is looking at absolute concentration values. The comparisons between BASCOE and FTIR do not show the systematic bias that is observed in the direct MIPAS-FTIR comparisons, except at Wollongong. The bias between BASCOE assimilation analyses for HNO_3 and the MIPAS HNO_3 data, discussed in Sect. 4 and shown in Fig. 4, is clearly seen in Figs. 9 and 10. Even if the products of BASCOE seem to be closer to the ground-based FTIR products, it is not possible to conclude that the MIPAS measurements of HNO_3 are too high. Still, BASCOE nicely reproduces the seasonal variation.

The second noticeable fact in Table 5 is that the standard deviations of all statistics are significantly larger than expected on the basis of the random uncertainties of the relative partial column differences which are only 3 or 4%. If the same spectroscopy would have been adopted for the MIPAS and FTIR retrievals, the standard deviation would decrease by a factor of 0.863. This would give, for “Statistics 4”, a standard deviation of 4% in the best case of Arrival Heights limited to the January-March period, up to 10% in the worst case of Arrival Heights when the whole year 2003 is considered. This means that additional unexpected random differences appear when comparing the FTIR and MIPAS products.

The additional uncertainties can largely be explained by the uncertainties due to spatial variability of HNO_3 . It is clearly seen in Table 5 by comparing “Statistics 1” and “2”, that a stricter collocation criterion reduces in a significant way the standard deviations. One could expect that the use of BASCOE would reduce the standard deviations to the level of the estimated random uncertainty, as observed for N_2O at the

Comparisons between g-b FTIR and MIPAS N_2O and HNO_3

C. Vigouroux et al.

[Title Page](#)[Abstract](#)[Introduction](#)[Conclusions](#)[References](#)[Tables](#)[Figures](#)[⏪](#)[⏩](#)[◀](#)[▶](#)[Back](#)[Close](#)[Full Screen / Esc](#)[Printer-friendly Version](#)[Interactive Discussion](#)

mid-latitude stations, but this is not the case, as shown by “Statistics 3” and “4” in the table. This means that the BASCOE resolution (5° in longitude and 3.75° in latitude) is not sufficient to reproduce the HNO_3 spatial variability, as it was the case for N_2O at high latitude during the period with high variability. We see in Fig. 4 that the standard deviations of the statistics on the differences between BASCOE and MIPAS are larger during the periods of higher variability (January to March for Kiruna, and September to November for Arrival Heights).

An additional, related contribution to the observed larger standard deviations comes from the so-called horizontal smearing effect, as follows. In reality, both the MIPAS and ground-based FTIR data stem from observations that are integrated measurements along their respective line-of-sights, that are oriented differently in space. Moreover, the sighted airmasses have a horizontal extension, that depends on the observation geometry and spectral characteristics, and that may become as large as 500 km. In other words, if the observed target species' concentration is non-uniform in space, over distances smaller than the sampling distances, the target species' abundances sampled by FTIR and MIPAS, and therefore also by BASCOE, may be different.

6.2.2 Comparisons of the vertical profiles of HNO_3

Figure 11 presents, for the five stations, the relative differences between the vertical profiles of HNO_3 for the two comparison ensembles, “Statistics 1” and “3”, analogously to Fig. 8 for N_2O .

The profiles comparisons confirm the conclusions as to bias and standard deviations discussed in the previous section. First, the expected positive bias between MIPAS and FTIR, due to the use of different spectroscopy, is observed in the profiles comparisons. The shape of the bias is different from station to station: it is mainly located at 100 hPa for Jungfraujoch and 30 hPa at Kiruna, whereas at Wollongong, Lauder and Arrival Heights (reduced period), the highest biases are observed at about 100 and 15 hPa. A similar shape for these three stations is not surprising as they used a similar retrieval strategy (choice of micro-windows, a priori covariance matrix,...). The DOFS

**Comparisons
between g-b FTIR and
MIPAS N_2O and HNO_3**

C. Vigouroux et al.

Title Page

Abstract

Introduction

Conclusions

References

Tables

Figures

◀

▶

◀

▶

Back

Close

Full Screen / Esc

Printer-friendly Version

Interactive Discussion

for the FTIR HNO₃ retrievals between the considered pressure limits is between 1.5 (for Jungfraujoch) and 2.4 (for Lauder); therefore, the detailed shape strongly depends on the retrieval settings. Second, we can see from the different biases obtained using BASCOE compared to the MIPAS ones, that the assimilation is not as good as for N₂O, as already discussed in Sect. 4. Third, we see that the estimated random error (shaded area) is lower than the standard deviations, as obtained for the partial columns, probably due to high spatial and temporal variability of HNO₃ and the horizontal smearing effect discussed in the previous section. At high altitude, the relative differences go to zero but not the random uncertainty because the error calculation uses, for all the stations, a typical averaging kernel matrix of Kiruna, which has a sensitivity different from zero even at high altitude.

7 Conclusions

Comparisons have been performed between MIPAS and ground-based FTIR vertical profiles of N₂O and HNO₃, covering the full year of 2003. The MIPAS data were provided by the ESA v4.61 data processor. The FTIR profiles have been retrieved at five NDACC sites distributed in latitude, namely Kiruna (68° N), Jungfraujoch (46.5° N), Wollongong (34° S), Lauder (45° S) and Arrival Heights (78° S). The consistency between the retrievals from the five stations has been optimised. For the first time, the same FTIR data have also been compared with corresponding results from the 4D-VAR data assimilation system BASCOE that were obtained in the configuration in which BASCOE assimilates the ESA v4.61 products for the six primary MIPAS species (H₂O, O₃, NO₂, HNO₃, CH₄, and N₂O). This was done to evaluate the impact of the spatial collocation criteria on the comparison results and to judge the appropriateness of using BASCOE results as proxies for MIPAS profiles in the stratosphere.

Considering the comparisons between the N₂O MIPAS and FTIR lower stratosphere partial columns during the year 2003, the biases are small and significant only for Wollongong (+4±2%) and Arrival Heights (-5±2%). The scatter is less than 7% for

**Comparisons
between g-b FTIR and
MIPAS N₂O and HNO₃**

C. Vigouroux et al.

Title Page

Abstract

Introduction

Conclusions

References

Tables

Figures

◀

▶

◀

▶

Back

Close

Full Screen / Esc

Printer-friendly Version

Interactive Discussion

**Comparisons
between g-b FTIR and
MIPAS N₂O and HNO₃**C. Vigouroux et al.

[Title Page](#)[Abstract](#)[Introduction](#)[Conclusions](#)[References](#)[Tables](#)[Figures](#)[◀](#)[▶](#)[◀](#)[▶](#)[Back](#)[Close](#)[Full Screen / Esc](#)[Printer-friendly Version](#)[Interactive Discussion](#)

the three mid-latitude stations and less than 10% for the high latitude ones. This was obtained using a coincidence criterion of 1000 km radius around the stations, and it has been demonstrated that the use of BASCOE reduces the collocation problem: the standard deviations between BASCOE and FTIR partial columns are less than 4% and 7% for the mid-latitude and high latitude stations, respectively. It has also been shown that, because the spatial resolution of the BASCOE data used here is limited to 5° longitude by 3.75° latitude, it represents less accurately the N₂O field in regions/periods with high temporal/spatial variability, such as in polar vortex conditions. Out of these periods, the standard deviation for the high latitude stations is also less than 4%, which is within the estimated random error. BASCOE profiles can indeed be considered to be good proxies for the MIPAS N₂O data. Concerning the N₂O profiles comparisons, we observed that the biases are quite low: below 5% for Kiruna, Lauder, and Arrival Heights during the reduced time period in the whole considered pressure range; below 5% and 10% at Jungfraujoch for pressure greater and lower than 20 hPa respectively; below 8% for Arrival Heights during the whole year 2003; below 5% at Wollongong for pressure greater than 5 hPa but a high bias (21%) is obtained at 25 hPa. The standard deviations are within the limits of uncertainty for pressure approximately greater than 100 hPa. For upper altitudes, the standard deviations are much larger than the estimated random error.

Regarding the comparisons of HNO₃ MIPAS and FTIR partial columns, a known bias, which is due to a scaling factor of 13% of the line-intensities in the different spectral databases, has been confirmed. Taking this fact into account, we would not have seen any statistically significant biases except at Arrival Heights (+6±3%). The standard deviations, corrected by the factor 0.863 for eliminating the effect of the different line-intensities, would be less than 15% at all stations except Arrival Heights where it would be 21%. These large standard deviations are clearly due to the too loose coincidence criterion of 1000 km. Considering the high spatial variability of HNO₃, even with a collocation of 400 km, the statistics of the comparisons show standard deviations that are larger (by about a factor 2 to 4) than expected on the basis of the random uncer-

tainty of the MIPAS-FTIR differences. This is explained by the fact that the HNO_3 fields exhibit variabilities on small (<400 km) spatial scales that cannot be distinguished in the comparisons because the collocation is never perfect.

The use of BASCOE instead of MIPAS profiles cannot completely solve the collocation problem because the spatial resolution of BASCOE is not sufficient and because, at present, the variations of the HNO_3 field across the horizontal extension of the probed airmasses, which we call the horizontal smearing effect, are not taken into account appropriately. Even if the standard deviations of comparisons between BASCOE and FTIR are not within the estimated random error, they are quite reasonable: after correction with the 0.863 factor, they are less than 10% for all the stations, during the whole year 2003. Concerning the biases between BASCOE and MIPAS, it turns out that in its present status, BASCOE does not provide as good proxies for the MIPAS HNO_3 profiles as for N_2O , because it uses assimilation convergence criteria that are too much relaxed.

This paper has also demonstrated that ground-based FTIR measurements, despite their low vertical resolution, are useful for satellite validation because they allow a statistical approach. They have been solicited for additional validation efforts including other independent data from balloon, aircraft and satellite.

Acknowledgements. The authors thank the European Commission, and the Belgian Federal Science Policy and ESA for funding this work through the projects UFTIR (EVK-2002-00159), and Prodex CINAMON (ESA contracts 15151 and 15064) and TASTE (ESA contract 18028/04/NL/AR), respectively. They also acknowledge their national authorities for supporting the observations and the many people who have participated to them. In addition, we wish to thank the Stiftungsrat of the Jungfrauoch for supporting the facilities allowing to perform long term and regular observations at that site. The authors are also grateful to M. Ridolfi (University of Bologne) and U. Cortesi (IFAC-CNR) for discussions on MIPAS errors, and J. C. Lambert and C. De Clercq (BIRA-IASB) for discussions on interpretations of the results.

Comparisons between g-b FTIR and MIPAS N_2O and HNO_3

C. Vigouroux et al.

[Title Page](#)[Abstract](#)[Introduction](#)[Conclusions](#)[References](#)[Tables](#)[Figures](#)[◀](#)[▶](#)[◀](#)[▶](#)[Back](#)[Close](#)[Full Screen / Esc](#)[Printer-friendly Version](#)[Interactive Discussion](#)

References

- Blom, C. E., Camy-Peyret, C., Catoire, V., Chance, K., Oelhaf, H., Ovarlez, J., Payan, S., Pirre, M., Piesch, C., and Wetzel, G.: Validation of MIPAS temperature profiles by stratospheric balloon and aircraft measurements, Proceedings of the Second Workshop on the Atmospheric Chemistry Validation of Envisat (ACVE-2), Frascati, 3–7 May 2004, ESA Special Publication SP-562, August 2004. [8338](#)
- Blumenstock, T., Mikuteit, S., Hase, F., Boyd, I., Calisesi, Y., De Clercq, C., Lambert, J.-C., Koopman, R., McDermid, S., Oltmans, S., Swart, D., Raffalski, U., Schets, H., De Muer, D., Steinbrecht, W., Stübi, R., and Wood, S.: Comparison of MIPAS O₃ profiles with ground-based measurements, Proceedings of the Second Workshop on the Atmospheric Chemistry Validation of Envisat (ACVE-2), Frascati, 3–7 May 2004, ESA Special Publication SP-562, August 2004a. [8338](#)
- Blumenstock, T., Mikuteit, S., Griesfeller, A., Hase, F., Koop, G., Kramer, I., Schneider, M., Fischer, H., Gil, M., Moreta, J. R., Navarro Coma, M., Raffalski, U., Cuevas, E., Dix, B., and Schwarz G.: Validation of MIPAS and SCIAMACHY data by ground based spectroscopy at Kiruna, Sweden, and Izaña, Tenerife Island (AOID-191), Proceedings of the Second Workshop on the Atmospheric Chemistry Validation of Envisat (ACVE-2), Frascati, 3–7 May 2004, ESA Special Publication SP-562, August 2004b. [8356](#)
- Calisesi Y., Soebijanta V. T., and van Oss R.: Regridding of remote soundings: Formulation and application to ozone profile comparison, J. Geophys. Res., 110, D23306, doi:10.1029/2005JD006122, 2005. [8349](#)
- Camy-Peyret, C., Payan, S., Dufour, G., Oelhaf, H., Wetzel, G., Stiller, G., Glatthor, N., Blumenstock, T., Blom, C. E., Keim, C., Mikuteit, S., Engel, A., Pirre, M., Moreau, G., Catoire, V., Bracher, A., Weber, M., and Bramstedt, K.: Validation of MIPAS CH₄ profiles by stratospheric balloon, aircraft, satellite and ground based measurements, Proceedings of the Second Workshop on the Atmospheric Chemistry Validation of Envisat (ACVE-2), Frascati, 3–7 May 2004, ESA Special Publication SP-562, August 2004a. [8338](#)
- Camy-Peyret, C., Dufour, G., Payan, S., Oelhaf, H., Wetzel, G., Stiller, G., Blumenstock, T., Blom, C. E., Guld, T., Glatthor, N., Engel, A., Pirre, M., Catoire, V., Moreau, G., De Mazière, M., Vigouroux, C., Mahieu, E., Cortesi, U., and Mencaraglia, F.: Validation of MIPAS N₂O profiles by stratospheric balloon, aircraft and ground based measurements, Proceedings of the Second Workshop on the Atmospheric Chemistry Validation of Envisat (ACVE-2),

Comparisons between g-b FTIR and MIPAS N₂O and HNO₃

C. Vigouroux et al.

Title Page

Abstract

Introduction

Conclusions

References

Tables

Figures

◀

▶

◀

▶

Back

Close

Full Screen / Esc

Printer-friendly Version

Interactive Discussion

- Frascati, 3–7 may 2004, ESA Special Publication SP-562, August 2004b. [8338](#)
- Cortesi, U., Blom, C. E., Camy-Peyret, C., Chance, K., Davies, J., Goutail, F., Kuttippurath, J., McElroy, C. T., Mencaraglia, F., Oelhaf, H., Petritoli, A., Pirre, M., Pommereau, J.-P., Ravegnani, F., Renard, J.-B., and Strong, K.: MIPAS ozone validation by stratospheric balloon and aircraft measurements, Proceedings of the Second Workshop on the Atmospheric Chemistry Validation of Envisat (ACVE-2), Frascati, 3–7 may 2004, ESA Special Publication SP-562, August 2004. [8338](#)
- Dethof, A., Geer, A., Lahoz, W., Goutail, F., Bazureau, A., Wang, D.-Y., and von Clarmann, T.: MIPAS temperature validation by the MASI group, Proceedings of the Second Workshop on the Atmospheric Chemistry Validation of Envisat (ACVE-2), Frascati, 3–7 May 2004, ESA Special Publication SP-562, August 2004. [8338](#)
- Errera, Q. and Fonteyn, D.: Four-dimensional variational chemical assimilation of CRISTA stratospheric measurements, *J. Geophys. Res.*, 106, 12 253–12 265, 2001. [8344](#)
- ESA, Envisat-MIPAS, An instrument for Atmospheric Chemistry and Climate Research, SP-1229, published by ESA Publications Division, ESTEC, P.O. Box 299, 2200 AG Noordwijk, The Netherlands, March 2000. [8337](#)
- ESA, Envisat-MIPAS Monthly report: March 2004, Technical Note, ENVI-SPPA-EOPG-TN-04-0011, May 2004. [8339](#)
- Fischer, H. and Oelhaf, H.: Remote sensing of vertical profiles of atmospheric trace constituents with MIPAS limb-emission spectrometers, *Appl. Opt.*, 35, 2787–2796, 1996. [8337](#)
- Fonteyn, D., Lahoz, W., Geer, A., Dethof, A., Wargan, K., Stajner, L., Pawson, S., Rood, R. B., Bonjean, S., Chabrillat, S., Daerden, F., and Errera, Q.: MIPAS ozone assimilation, Proceedings of the Second Workshop on the Atmospheric Chemistry Validation of Envisat (ACVE-2), Frascati, 3–7 may 2004, ESA Special Publication SP-562, August 2004. [8338](#)
- Fricke, K. H., Blum, U., Baumgarten, G., Congeduti, F., Cuomo, V., Hansen, G., Mona, L., Schets, H., Stebel, K., and Stübi, R.: MIPAS temperature validation with radiosonde and lidar, Proceedings of the Second Workshop on the Atmospheric Chemistry Validation of Envisat (ACVE-2), Frascati, 3–7 May 2004, ESA Special Publication SP-562, August 2004. [8338](#), [8340](#)
- Geer, A. J., Lahoz, W. A., Bekki, S., et al.: The ASSET intercomparison of ozone analyses: method and first results, *Atmos. Chem. Phys. Discuss.*, 6, 4495–4577, 2006.
- Hase, F.: Inversion von Spurengasprofilen aus hochaufgelösten bodengebundenen FTIR-Messungen in absorption. Wissenschaftliche Berichte Forschungszentrum Karlsruhe, FZKA

**Comparisons
between g-b FTIR and
MIPAS N₂O and HNO₃**C. Vigouroux et al.

Title Page

Abstract

Introduction

Conclusions

References

Tables

Figures

◀

▶

◀

▶

Back

Close

Full Screen / Esc

Printer-friendly Version

Interactive Discussion

6512; ISSN 0947-8620, 2000. [8340](#)

Hase, F., Hannigan, J. W., Coffey, M. T., Goldman, A., Höpfner, M., Jones, N. B., Rinsland, C. P., and Wood, S. W.: Intercomparison of retrieval codes used for the analysis of high-resolution, ground-based FTIR measurements, *J. Quant. Spectros. Radiat. Transfer*, 87, 25-52, 2004.

[8340](#)

Kerridge, B. J., Goutail, F., Bazureau, A., Wang, D.-Y., Bracher, A., Weber, M., Bramstedt, K., Siddans, R., Latter, B. G., Reburn, W. J., Jay, V. L., Dethof, A., and Payne V. H.: MIPAS ozone validation by satellite intercomparisons, Proceedings of the Second Workshop on the Atmospheric Chemistry Validation of Envisat (ACVE-2), Frascati, 3–7 may 2004, ESA Special Publication SP-562, August 2004. [8338](#)

Lahoz, W., Geer, A., Swinbank, R., Jackson, D., Thornton, H., Dethof, A., and Fonteyn, D.: Modelling and assimilation: evaluation of MIPAS water vapour data, Proceedings of the Second Workshop on the Atmospheric Chemistry Validation of Envisat (ACVE-2), Frascati, 3–7 may 2004, ESA Special Publication SP-562, August 2004. [8338](#)

Meier, A., Toon, G. C., Rinsland, C. P., Goldman, A., and Hase, F.: Spectroscopic Atlas of Atmospheric Microwindows in the middle Infra-Red, IRF Technical Report 048, ISSN 0284-1738 (Institutet för Rymdfysik, Kiruna, Sweden), Appendix E, 2004. [8341](#)

Ménard, R., Cohn, S. E., Chang, L. P., and Lyster, P. M.: Assimilation of Stratospheric Chemical Tracer Observations Using a Kalman Filter. Part I: Formulation, *Mon. Weather Rev.*, 128, 2654–2671, 2000. [8345](#)

Oelhaf, H., Fix, A., Schiller, C., Chance, K., Gurlit, W., Ovarlez, J., Renard, J.-B., Rohs, S., Wetzel, G., von Clarmann, T., Milz, M., Wang, D.-Y., Remedios, J. J., and Waterfall, A. M.: Validation of MIPAS-ENVISAT version 4.61 operational data with balloon and aircraft measurements: H₂O, Proceedings of the Second Workshop on the Atmospheric Chemistry Validation of Envisat (ACVE-2), Frascati, 3–7 May 2004, ESA Special Publication SP-562, August 2004a. [8338](#)

Oelhaf, H., Blumenstock, T., De Mazière, M., Mikuteit, S., Vigouroux, C., Wood, S., Bianchini, G., Baumann, R., Blom, C., Cortesi, U., Liu, G. Y., Schlager, H., Camy-Peyret, C., Catoire, V., Pirre, M., Strong, K., and Wetzel, G.: Validation of MIPAS-ENVISAT version 4.61 HNO₃ operational data by stratospheric balloon, aircraft and ground based measurements, Proceedings of the Second Workshop on the Atmospheric Chemistry Validation of Envisat (ACVE-2), Frascati, 3–7 May 2004, ESA Special Publication SP-562, August 2004b. [8338](#), [8356](#)

ACPD

6, 8335–8382, 2006

**Comparisons
between g-b FTIR and
MIPAS N₂O and HNO₃**

C. Vigouroux et al.

Title Page

Abstract

Introduction

Conclusions

References

Tables

Figures

◀

▶

◀

▶

Back

Close

Full Screen / Esc

Printer-friendly Version

Interactive Discussion

EGU

Pappalardo, G., Colavitto, T., Congeduti, F., Cuomo, V., Deuber, B., Kämpfer, N., Iarlori, M., Mona, L., and Rizi, V.: Validation of MIPAS water vapour products by ground-based measurements, Proceedings of the Second Workshop on the Atmospheric Chemistry Validation of Envisat (ACVE-2), Frascati, 3–7 May 2004, ESA Special Publication SP-562, August 2004.

8338

Pougatchev, N. S. and Rinsland, C. P.: Spectroscopic study of the seasonal variation of carbon monoxide vertical distribution above Kitt Peak., J. Geophys. Res., 100, 1409–1416, 1995a.

8340

Pougatchev, N. S., Connor, B. J., and Rinsland, C. P.: Infrared measurements of the ozone vertical distribution above Kitt Peak, J. Geophys. Res., 100, 16 689–16 697, 1995b.

8340

Rinsland, C. P., Jones, N. B., Connor, B. J., Logan, J. A., Goldman, A., Murcray, F. J., Stephen, T. M., Pougatchev, N. S., Zander, R., Demoulin, P., and Mahieu, E.: Northern and southern hemisphere ground-based infrared measurements of tropospheric carbon monoxide and ethane, J. Geophys. Res., 103, 28 197–28 217, 1998.

8340

Rodgers, C. D.: Inverse methods for atmospheric sounding: Theory and Practice, Series on Atmospheric, Oceanic and Planetary Physics – Vol. 2, World Scientific Publishing Co., Singapore, 2000.

8337, 8340, 8342

Rodgers, C. D. and Connor, B. J.: Intercomparison of remote sounding instruments, J. Geophys. Res., 108, 4116–4129, 2003.

8346, 8349

Rothman, L. S., Barbe, A., Chris Benner, D., Brown, L. R., Camy-Peyret, C., Carleer, M. R., Chance, K., Clerbaux, C., Dana, V., Devi, V. M., Fayt, A., Flaud, J.-M., Gamache, R. R., Goldman, A., Jacquemart, D., Jucks, K. W., Lafferty, W. J., Mandin, J.-Y., Massie, S. T., Nemtchinov, V., Newnham, D. A., Perrin, A., Rinsland, C. P., Schroeder, J., Smith, K. M., Smith, M. A. H., Tang, K., Toth, R. A., Vander Auwera, J., Varanasi, P., and Yoshino, K.: The HITRAN molecular spectroscopic database: Edition of 2000 including updates through 2001, J. Quant. Spectros. Radiat. Transfer, 82, 5–44, 2003.

8341

Weber, M., Bracher, A., Bramstedt, K., Bazureau, A., and Goutail, F.: Overview on validation of MIPAS H₂O vapour by comparison with independent satellite measurements, Proceedings of the Second Workshop on the Atmospheric Chemistry Validation of Envisat (ACVE-2), Frascati, 3–7 May 2004, ESA Special Publication SP-562, August 2004.

8338

Wetzel, G., Blumenstock, T., Oelhaf, H., Stiller, G. P., Wang, D.-Y., Zhang, G., Pirre, M., Goutail, F., Bazureau, A., Pommereau, J.-P., Bracher, A., Sinnhuber, M., Weber, M., Bramstedt, K., Funke, B., López-Puertas, M., Kostadinov, I., Petritoli, A., Alfaro, A., Hendrick, F., Van

ACPD

6, 8335–8382, 2006

**Comparisons
between g-b FTIR and
MIPAS N₂O and HNO₃**

C. Vigouroux et al.

Title Page

Abstract

Introduction

Conclusions

References

Tables

Figures

◀

▶

◀

▶

Back

Close

Full Screen / Esc

Printer-friendly Version

Interactive Discussion

EGU

Rozendael, M., and De Mazière, M.: Validation of MIPAS-ENVISAT version 4.61 operational data: NO₂, Proceedings of the Second Workshop on the Atmospheric Chemistry Validation of Envisat (ACVE-2), Frascati, 3–7 May 2004, ESA Special Publication SP-562, August 2004. [8338](#)

ACPD

6, 8335–8382, 2006

**Comparisons
between g-b FTIR and
MIPAS N₂O and HNO₃**

C. Vigouroux et al.

Title Page

Abstract

Introduction

Conclusions

References

Tables

Figures

⏪

⏩

◀

▶

Back

Close

Full Screen / Esc

Printer-friendly Version

Interactive Discussion

EGU

Comparisons between g-b FTIR and MIPAS N₂O and HNO₃

C. Vigouroux et al.

Table 1. Spectral microwindows (cm⁻¹) used for the ground-based FTIR retrievals.

| Station | N ₂ O | | HNO ₃ | |
|--------------------------|--|--|--|--|
| | Microwindow limits (cm ⁻¹) | Interfering species | Microwindow limits (cm ⁻¹) | Interfering species |
| Kiruna | 2481.3–2482.6 | CO ₂ , CH ₄ , H ₂ O, O ₃ | 867.0–869.6 | OCS, H ₂ O, CO ₂ , C ₂ H ₆ , CCl ₂ F ₂ |
| | 2526.4–2528.2 | CO ₂ , CH ₄ , H ₂ O, O ₃ | 872.8–875.2 | OCS, H ₂ O, CO ₂ , C ₂ H ₆ , CCl ₂ F ₂ |
| | 2537.85–2538.8 | CO ₂ , CH ₄ , H ₂ O, O ₃ | | |
| | 2540.1–2540.7 | CO ₂ , CH ₄ , H ₂ O, O ₃ | | |
| Jungfraujoch | 2481.3–2482.6 | CO ₂ , CH ₄ | 868.476–870 | OCS, H ₂ O |
| | 2526.4–2528.2 | CO ₂ , CH ₄ , HDO | | |
| | 2537.85–2538.8 | CH ₄ | | |
| | 2540.1–2540.7 | none | | |
| Wollongong | 2481.2–2483.5 | CO ₂ , CH ₄ | 868.47–870 | OCS, H ₂ O, NH ₃ , CO ₂ |
| | | | 872.8 – 874.0 | OCS, H ₂ O, NH ₃ , CO ₂ |
| Lauder & Arrival Heights | 2481.2–2483.5 | CO ₂ , CH ₄ | 868.3–869.6 | OCS, H ₂ O, NH ₃ |
| | | | 872.8 – 874.0 | OCS, H ₂ O, NH ₃ |

Title Page

Abstract

Introduction

Conclusions

References

Tables

Figures

◀

▶

◀

▶

Back

Close

Full Screen / Esc

Printer-friendly Version

Interactive Discussion

Comparisons between g-b FTIR and MIPAS N₂O and HNO₃

C. Vigouroux et al.

Table 2. Characterization of the retrieved profiles of N₂O and HNO₃ at each station: statistical mean and standard deviation (1σ) for one year of measurements of the Degrees of Freedom for Signal (DOFS), and Sensitivity Range (S.R.) of the ground-based FTIR retrievals (Gd: ground).

| Station | N ₂ O | | HNO ₃ | |
|-----------------|------------------|--------------|------------------|--------------|
| | DOFS | S.R. (km) | DOFS | S.R. (km) |
| Kiruna | 3.6±0.2 | Gd–25 | 2.5±0.5 | 13–36 |
| Jungfrauoch | 4.3±0.2 | Gd–45 | 1.9±0.4 | 10–27 |
| Wollongong | 3.5±0.2 | Gd–30 | 2.1±0.4 | 14–32 |
| Lauder | 3.7±0.3 | Gd–30 | 2.8±0.3 | 8–34 |
| Arrival Heights | 3.7±0.2 | Gd–28 | 2.8±0.4 | 8–34 |

[Title Page](#)
[Abstract](#)
[Introduction](#)
[Conclusions](#)
[References](#)
[Tables](#)
[Figures](#)
[Back](#)
[Close](#)
[Full Screen / Esc](#)
[Printer-friendly Version](#)
[Interactive Discussion](#)

Comparisons between g-b FTIR and MIPAS N₂O and HNO₃

C. Vigouroux et al.

Table 3. Statistical means and standard deviations [$\langle X\text{-FTIR} \rangle \pm 1\sigma / \langle \text{FTIR} \rangle$] [%] of the N₂O partial columns confined between the given pressure limits. X stands for the MIPAS partial columns collocated within 1000 km (“Statistics 1”) and 400 km (“Statistics 2”) around the ground-based stations, or, the BASCOE partial columns corresponding to cases where MIPAS data exist within the adopted collocation times (“Statistics 3”) and for all cases where FTIR ground-based data exist (“Statistics 4”). All X profiles have been smoothed by the ground-based FTIR averaging kernel matrices as explained in Sect. 5.1. The numbers of comparisons included in the different statistics are given between parentheses.

| N ₂ O | | [$\langle \text{MIPAS-FTIR} \rangle \pm 1\sigma / \langle \text{FTIR} \rangle$] | | | [$\langle \text{BASCOE-FTIR} \rangle \pm 1\sigma / \langle \text{FTIR} \rangle$] | | |
|-------------------------|-----------------------|---|--------------------|-------------------------------|--|--------------------|--|
| Station | Pressure limits [hPa] | “Statistics 1” [%] | “Statistics 2” [%] | Random error ^α [%] | “Statistics 3” [%] | “Statistics 4” [%] | |
| Kiruna (68° N) | 182–24 | −1±9 (283) | −4±9 (6) | 6 | +0±7 (86) | +0±7 (119) | |
| Jungfraujoch (46.5° N) | 198–1 | +2±6 (130) | +1±3 (10) | 6 | +0±2 (64) | +0±2 (176) | |
| Wollongong (34° S) | 207–12 | +4±7 (78) | +9±10 (4) | 6 | +0±3 (31) | −1±3 (133) | |
| Lauder (45° S) | 199–12 | +0±7 (194) | +4±5 (11) | 6 | +0±4 (89) | +1±4 (273) | |
| Arrival Heights (78° S) | 181–17 | −5±10 (271) | −8±9 (24) | 7 | −5±6 (48) | −4±8 (70) | |

^αSee Sect. 5.3 for the estimation of the error on the relative differences.

Title Page

Abstract

Introduction

Conclusions

References

Tables

Figures

◀

▶

◀

▶

Back

Close

Full Screen / Esc

Printer-friendly Version

Interactive Discussion

Comparisons between g-b FTIR and MIPAS N₂O and HNO₃

C. Vigouroux et al.

Table 4. Same as Table 3 but for a reduced (summer-autumn) time period, at Kiruna and Arrival Heights.

| Station | N ₂ O Pressure limits [hPa] | [<MIPAS-FTIR>±1σ]/<FTIR> | | | [<BASCOE-FTIR>±1σ]/<FTIR> | | |
|----------------------------|--|--------------------------|-----------------------|---------------------|---------------------------|-----------------------|--|
| | | “Statistics 1” [%] | “Statistics 2” [%] | Random error [%] | “Statistics 3” [%] | “Statistics 4” [%] | |
| Kiruna, June–Oct | 182–24 | +1±5 (187) | +1±4 (4) | 6 | +0±3 (54) | +0±2 (67) | |
| Arrival Heights, Jan–March | 181–17 | −4±5 (126) | −4±4 (10) | 6 | −1±3 (19) | −1±3 (31) | |

Title Page

Abstract

Introduction

Conclusions

References

Tables

Figures

◀

▶

◀

▶

Back

Close

Full Screen / Esc

Printer-friendly Version

Interactive Discussion

Comparisons between g-b FTIR and MIPAS N₂O and HNO₃

C. Vigouroux et al.

Table 5. Statistical means and standard deviations [$\langle X\text{-FTIR} \rangle \pm 1\sigma / \langle \text{FTIR} \rangle$ [%] of the HNO₃ partial columns confined between the given pressure limits. X stands for the MIPAS partial columns collocated within 1000 km (“Statistics 1”) and 400 km (“Statistics 2”) around the ground-based stations, or, the BASCOE partial columns corresponding to cases where MIPAS data exist within the adopted collocations times (“Statistics 3”) and for all cases where FTIR ground-based data exist (“Statistics 4”). All X profiles have been smoothed by the ground-based FTIR averaging kernel matrices as explained in Sect. 5.1. The numbers of comparisons included in the different statistics are given between parentheses. K.: Kiruna; A.H.: Arrival Heights.

| Station | HNO ₃ Pressure limits [hPa] | $\langle \text{MIPAS-FTIR} \rangle \pm 1\sigma / \langle \text{FTIR} \rangle$ | | | $\langle \text{BASCOE-FTIR} \rangle \pm 1\sigma / \langle \text{FTIR} \rangle$ | | |
|------------------|--|---|-----------------------|---------------------|--|-----------------------|--|
| | | “Statistics 1” [%] | “Statistics 2” [%] | Random error [%] | “Statistics 3” [%] | “Statistics 4” [%] | |
| Kiruna | 132–4 | +12±12 (362) | +20±7 (6) | 3 | +5±7 (91) | +5±9 (126) | |
| K., June-Oct | | +13±9 (248) | +18±6 (4) | 3 | +4±6 (61) | +5±6 (74) | |
| Jungfrauoch | 145–15 | +16±17 (167) | +14±12 (14) | 4 | +6±7 (60) | +5±8 (165) | |
| Wollongong | 151–9 | +11±17 (62) | +10±3 (2) | 4 | +12±10 (26) | +10±9 (131) | |
| Lauder | 144–7 | +15±13 (132) | +17±7 (9) | 3 | +4±8 (46) | +2±9 (138) | |
| Arrival Heights | 135–7 | +19±23 (318) | +17±14 (33) | 3 | +1±13 (51) | +2±12 (68) | |
| A. H., Jan-March | | +20±9 (126) | +19±5 (10) | 3 | +12±4 (19) | +11±5 (28) | |

Title Page

Abstract

Introduction

Conclusions

References

Tables

Figures

◀

▶

◀

▶

Back

Close

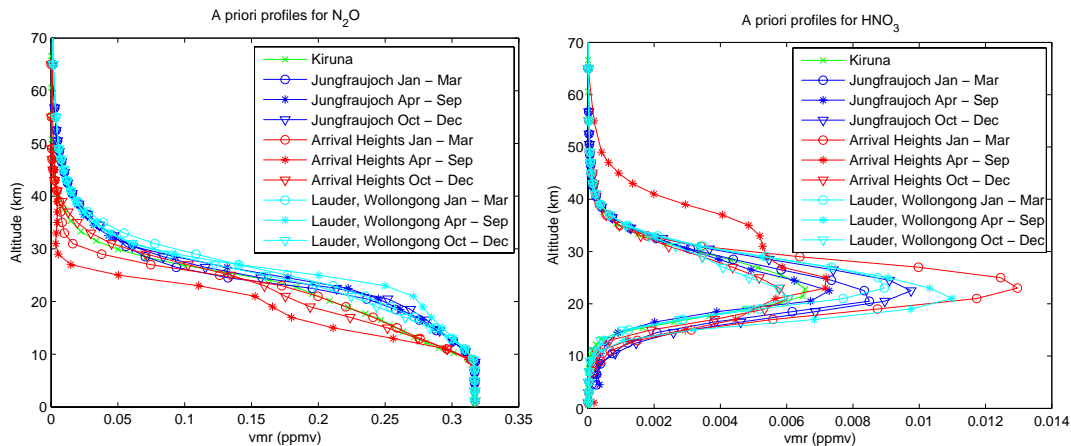
Full Screen / Esc

Printer-friendly Version

Interactive Discussion

**Comparisons
between g-b FTIR and
MIPAS N₂O and HNO₃**

C. Vigouroux et al.

**Fig. 1.** N₂O and HNO₃ a priori profiles at all stations.

Title Page

Abstract

Introduction

Conclusions

References

Tables

Figures

◀

▶

◀

▶

Back

Close

Full Screen / Esc

Printer-friendly Version

Interactive Discussion

**Comparisons
between g-b FTIR and
MIPAS N₂O and HNO₃**C. Vigouroux et al.

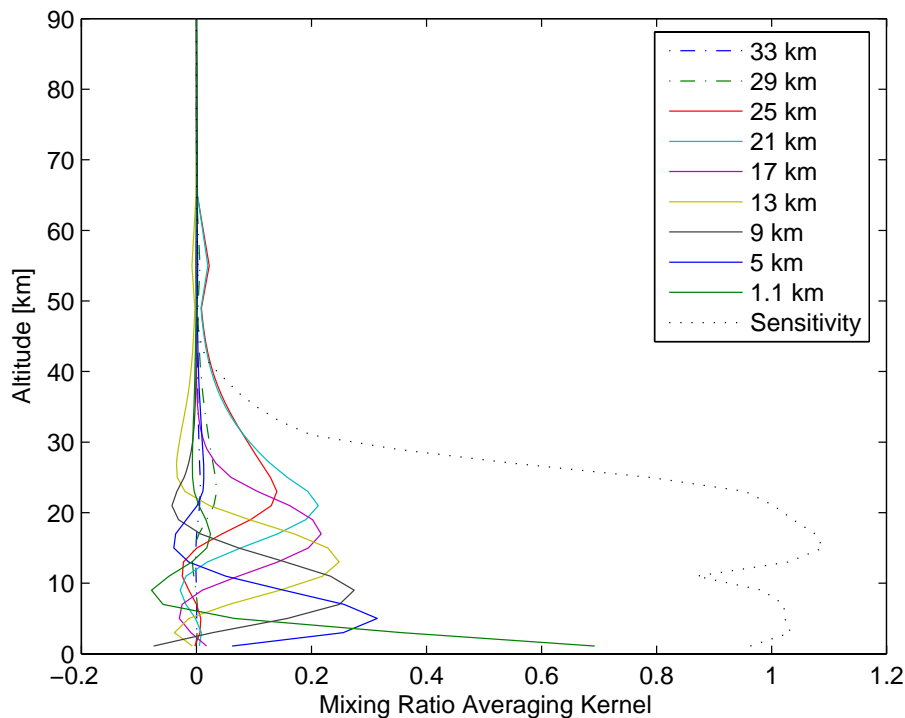


Fig. 2. Characterization of the retrieval of N₂O at Arrival Heights. Full lines: Averaging Kernels for the altitudes listed in the legend. Dotted line: Sensitivity of the retrieval as a function of altitude.

[Title Page](#)[Abstract](#)[Introduction](#)[Conclusions](#)[References](#)[Tables](#)[Figures](#)[◀](#)[▶](#)[◀](#)[▶](#)[Back](#)[Close](#)[Full Screen / Esc](#)[Printer-friendly Version](#)[Interactive Discussion](#)

**Comparisons
between g-b FTIR and
MIPAS N₂O and HNO₃**

C. Vigouroux et al.

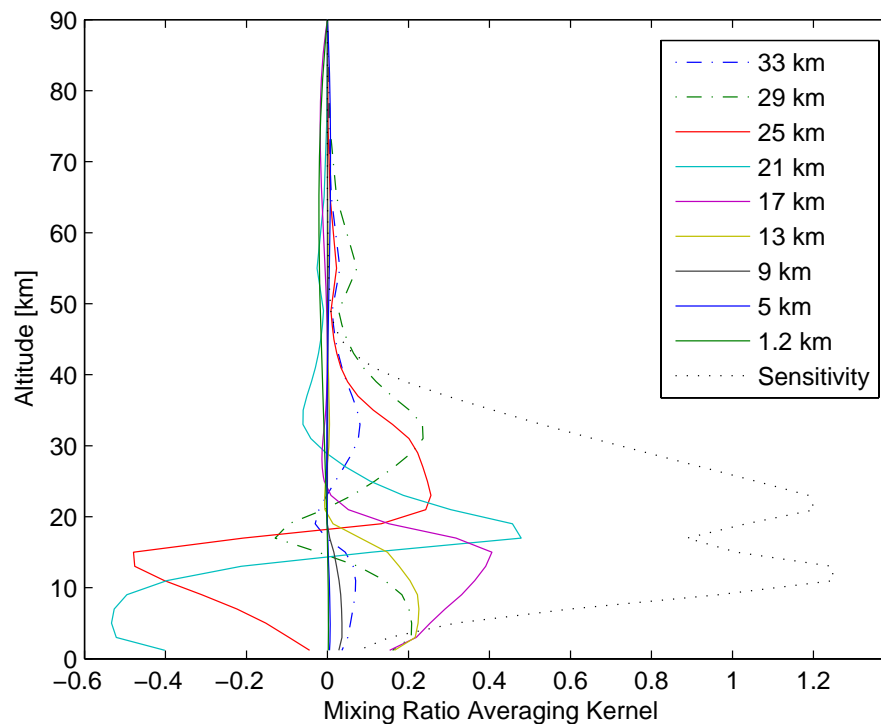


Fig. 3. Characterization of the retrieval of HNO₃ at Lauder. Full lines: Averaging Kernels for the altitudes listed in the legend. Dotted line: Sensitivity of the retrieval as a function of altitude.

[Title Page](#)[Abstract](#)[Introduction](#)[Conclusions](#)[References](#)[Tables](#)[Figures](#)[◀](#)[▶](#)[◀](#)[▶](#)[Back](#)[Close](#)[Full Screen / Esc](#)[Printer-friendly Version](#)[Interactive Discussion](#)

Comparisons between g-b FTIR and MIPAS N₂O and HNO₃

C. Vigouroux et al.

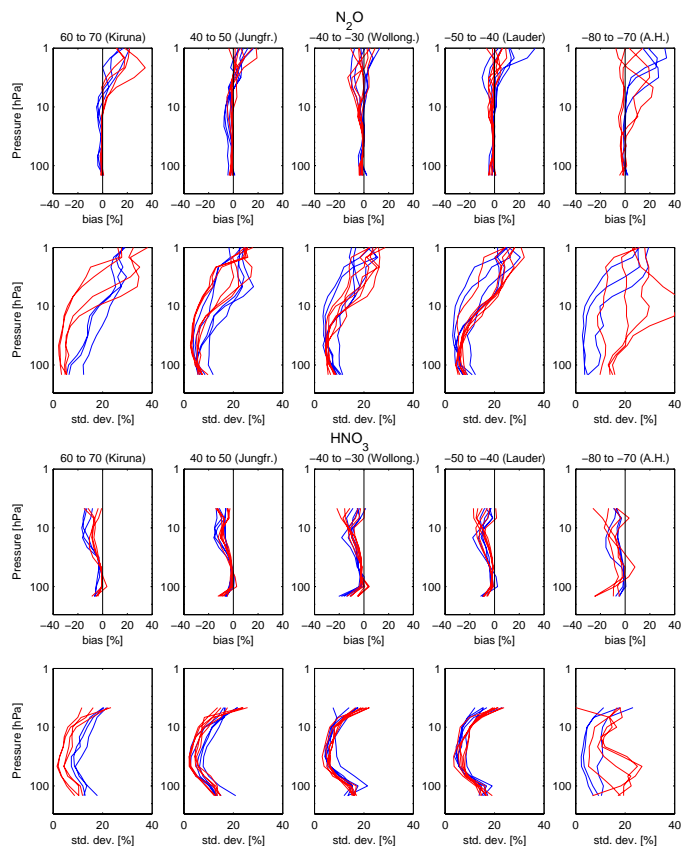


Fig. 4. Monthly zonal mean bias and standard deviation (std. dev.) between BASCOE and MIPAS profiles of N₂O (top) and HNO₃ (bottom), in 10° latitude bands around ground-based stations (A.H.: Arrival Heights). In blue: December to May; in red: June to November. For polar regions, monthly statistics are shown only for months where FTIR provides observations. Latitude are specified in °N.

Title Page

Abstract

Introduction

Conclusions

References

Tables

Figures

◀

▶

◀

▶

Back

Close

Full Screen / Esc

Printer-friendly Version

Interactive Discussion

**Comparisons
between g-b FTIR and
MIPAS N₂O and HNO₃**

C. Vigouroux et al.

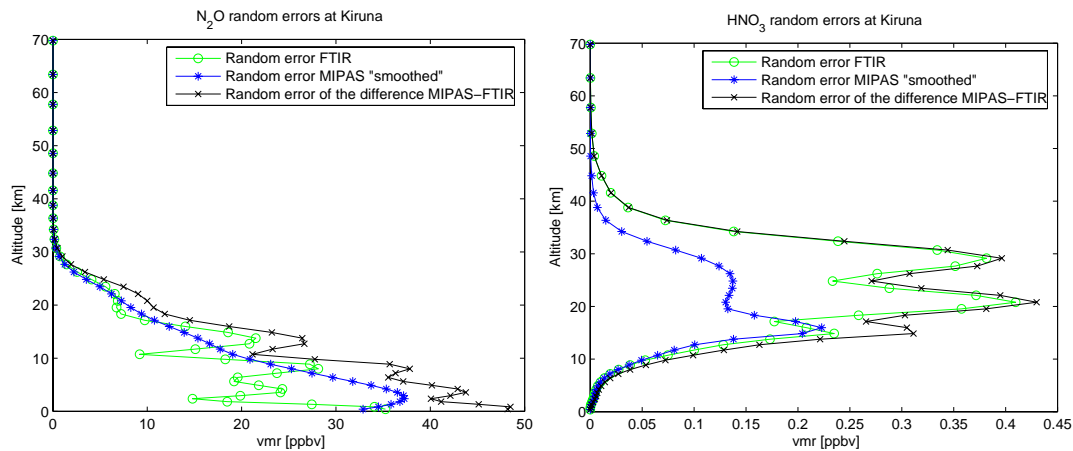


Fig. 5. Ground-based FTIR, MIPAS and (MIPAS-FTIR) random errors (in ppbv) for the N₂O (top) and HNO₃ (bottom) retrievals at Kiruna.

[Title Page](#)[Abstract](#)[Introduction](#)[Conclusions](#)[References](#)[Tables](#)[Figures](#)[◀](#)[▶](#)[◀](#)[▶](#)[Back](#)[Close](#)[Full Screen / Esc](#)[Printer-friendly Version](#)[Interactive Discussion](#)

**Comparisons
between g-b FTIR and
MIPAS N₂O and HNO₃**

C. Vigouroux et al.

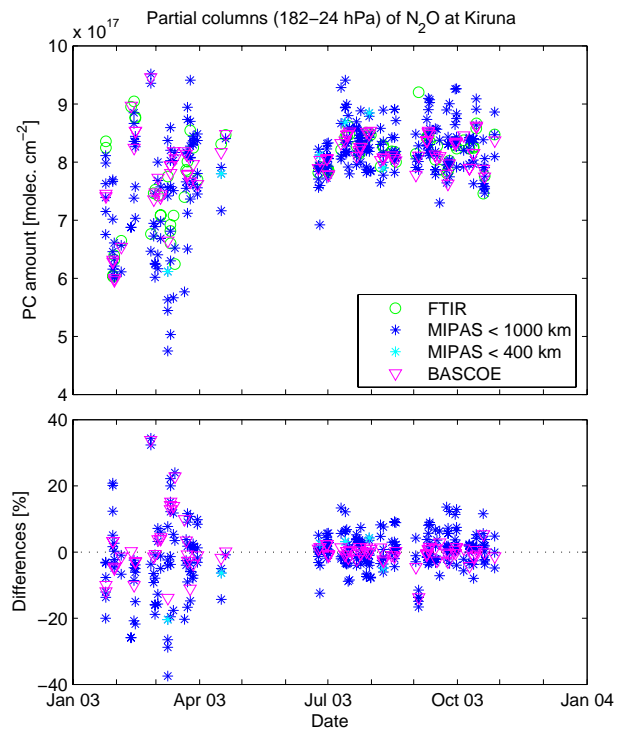


Fig. 6. Upper panel: Partial columns (182–24 hPa) of N₂O at Kiruna, from ground-based FTIR (green circles), MIPAS (dark blue and light blue stars for selections according to the spatial collocation criteria of 1000 and 400 km, respectively) and BASCOE (magenta triangles) data. Lower panel: Relative partial column differences (MIPAS-FTIR)/<FTIR> (stars; same colour coding as for upper plot), and (BASCOE-FTIR)/<FTIR> (magenta triangles).

[Title Page](#)[Abstract](#)[Introduction](#)[Conclusions](#)[References](#)[Tables](#)[Figures](#)[◀](#)[▶](#)[◀](#)[▶](#)[Back](#)[Close](#)[Full Screen / Esc](#)[Printer-friendly Version](#)[Interactive Discussion](#)

**Comparisons
between g-b FTIR and
MIPAS N₂O and HNO₃**

C. Vigouroux et al.

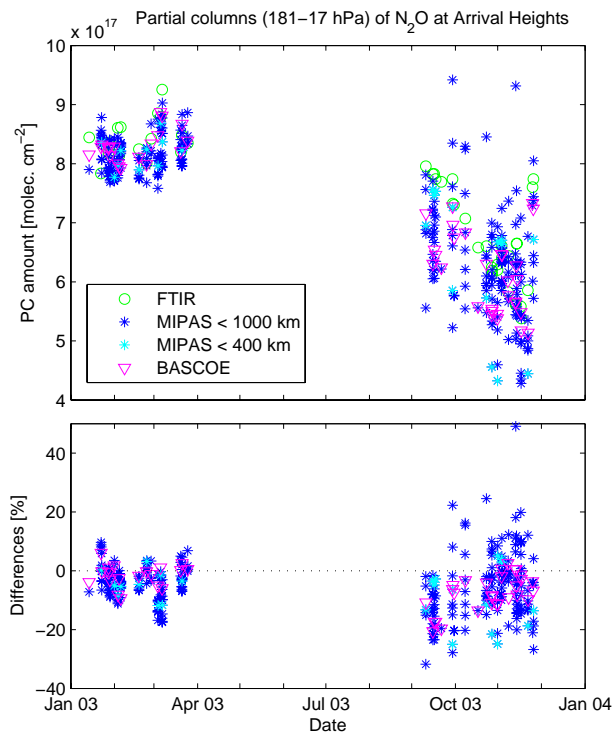


Fig. 7. Upper panel: Partial columns (181–17 hPa) of N₂O at Arrival Heights, from ground-based FTIR (green circles), MIPAS (dark blue and light blue stars for selections according to the spatial collocation criteria of 1000 and 400 km, respectively) and BASCOE (magenta triangles) data. Lower panel: Relative partial column differences (MIPAS-FTIR)/<FTIR> (stars; same colour coding as for upper plot), and (BASCOE-FTIR)/<FTIR> (magenta triangles).

[Title Page](#)[Abstract](#)[Introduction](#)[Conclusions](#)[References](#)[Tables](#)[Figures](#)[◀](#)[▶](#)[◀](#)[▶](#)[Back](#)[Close](#)[Full Screen / Esc](#)[Printer-friendly Version](#)[Interactive Discussion](#)

Comparisons between g-b FTIR and MIPAS N₂O and HNO₃

C. Vigouroux et al.

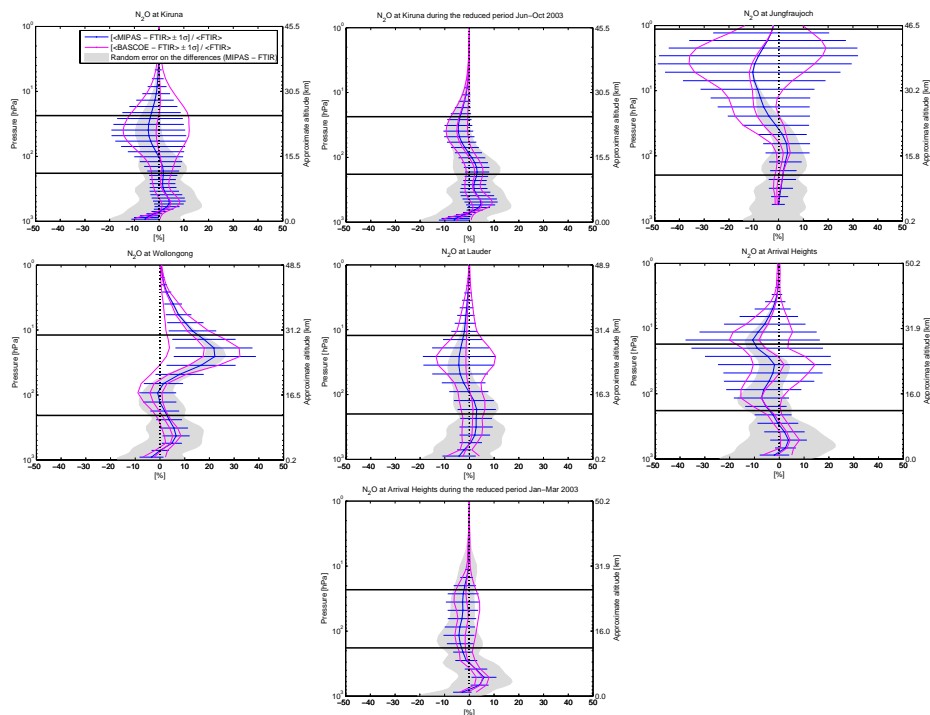


Fig. 8. Statistical means and standard deviations $[\langle X-FTIR \rangle \pm 1\sigma] / \langle FTIR \rangle$ [%] of the N₂O difference profiles. X represents the MIPAS collocated scans within 1000 km around the stations (“Statistics 1”, in blue) or the BASCOE correlative profiles (“Statistics 3”, in magenta). All X profiles have been smoothed by the ground-based FTIR averaging kernel matrices as discussed in Sect. 5.1. The numbers of coincidences included in both comparison data sets are given in Table 3. The black horizontal bars indicate the pressure limits of the partial columns defined before (see also Table 3). The shaded area represents the random uncertainty on the differences, in % (see Sect. 5.3).

Title Page

Abstract

Introduction

Conclusions

References

Tables

Figures

◀

▶

◀

▶

Back

Close

Full Screen / Esc

Printer-friendly Version

Interactive Discussion

**Comparisons
between g-b FTIR and
MIPAS N₂O and HNO₃**

C. Vigouroux et al.

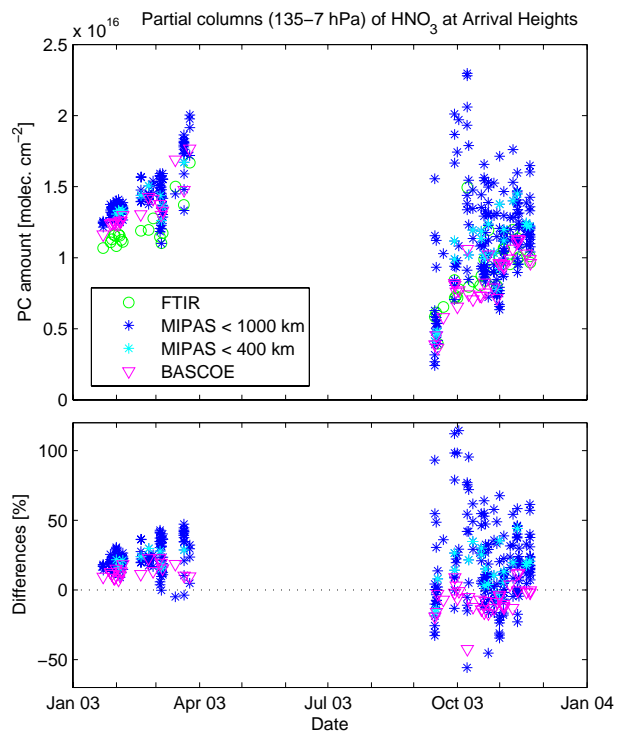


Fig. 9. Upper panel: Partial columns (135–7 hPa) of HNO₃ at Arrival Heights, from ground-based FTIR (green circles), MIPAS (dark blue and light blue stars for selections according to the spatial collocation criteria of 1000 and 400 km, respectively) and BASCOE (magenta triangles) data. Lower panel: Relative partial column differences (MIPAS-FTIR)/<FTIR> (stars; same colour coding as for upper plot), and (BASCOE-FTIR)/<FTIR> (magenta triangles).

[Title Page](#)[Abstract](#)[Introduction](#)[Conclusions](#)[References](#)[Tables](#)[Figures](#)[◀](#)[▶](#)[◀](#)[▶](#)[Back](#)[Close](#)[Full Screen / Esc](#)[Printer-friendly Version](#)[Interactive Discussion](#)

**Comparisons
between g-b FTIR and
MIPAS N₂O and HNO₃**

C. Vigouroux et al.

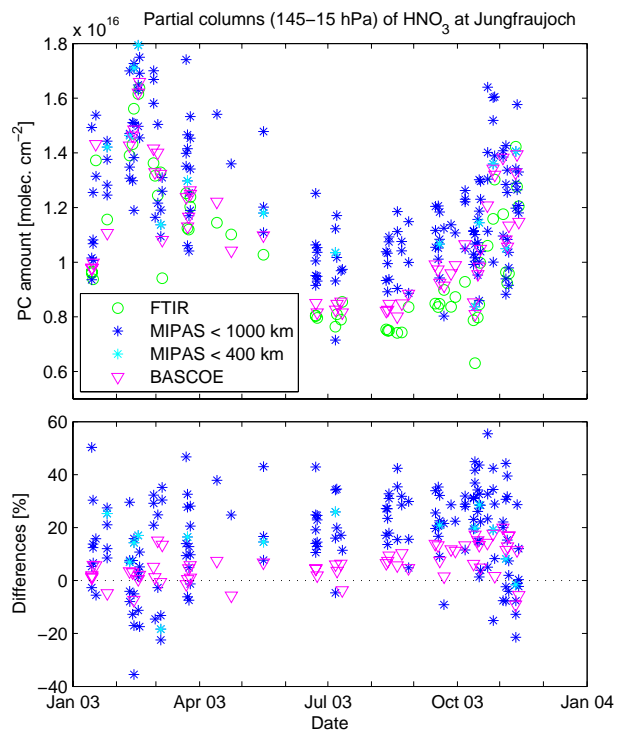


Fig. 10. Upper panel: Partial columns (145–15 hPa) of HNO₃ at the Jungfraujoch, from ground-based FTIR (green circles), MIPAS (dark blue and light blue stars for selections according to the spatial collocation criteria of 1000 and 400 km, respectively) and BASCOE (magenta triangles) data. Lower panel: Relative partial column differences (MIPAS-FTIR)/<FTIR> (stars; same colour coding as for upper plot), and (BASCOE-FTIR)/<FTIR> (magenta triangles).

[Title Page](#)[Abstract](#)[Introduction](#)[Conclusions](#)[References](#)[Tables](#)[Figures](#)[◀](#)[▶](#)[◀](#)[▶](#)[Back](#)[Close](#)[Full Screen / Esc](#)[Printer-friendly Version](#)[Interactive Discussion](#)

Comparisons between g-b FTIR and MIPAS N₂O and HNO₃

C. Vigouroux et al.

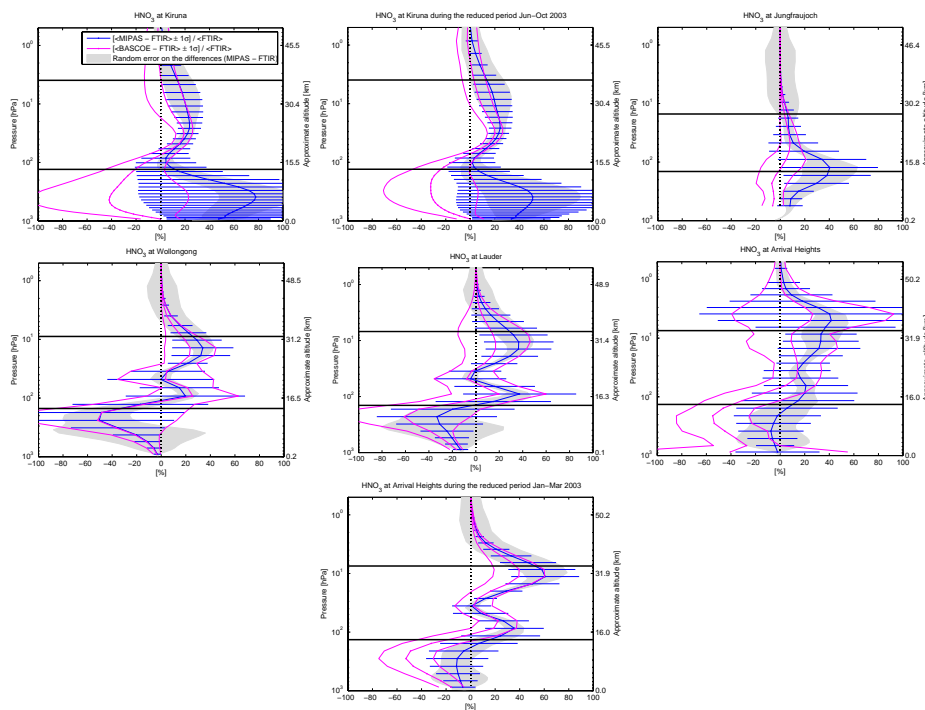


Fig. 11. Statistical means and standard deviations $[\langle X-FTIR \rangle \pm 1\sigma] / \langle FTIR \rangle$ [%] of the HNO₃ difference profiles. X represents the MIPAS collocated scans within 1000 km around the stations (“Statistics 1”, in blue) or the BASCOE correlative profiles (“Statistics 3”, in magenta). All X profiles have been smoothed by the ground-based FTIR averaging kernel matrices as discussed in Sect. 5.1. The numbers of coincidences included in both comparison data sets are given in columns 1 and 3 of Table 5. The black horizontal bars indicate the pressure limits of the partial columns defined before (see also Table 5). The shaded area represents the random uncertainty on the differences, in % (see Sect. 5.3).

Title Page

Abstract

Introduction

Conclusions

References

Tables

Figures

◀

▶

◀

▶

Back

Close

Full Screen / Esc

Printer-friendly Version

Interactive Discussion